Idaho National Engineering and Environmental Laboratory
INEEL/EXT-98-00964

September 1998

Engineered Barrier Testing at the INEEL Engineered Barriers Test Facility: FY-1997 and FY-1998

Indrek Porro
Karen N. Keck

LOCKHEED MARTIN

INEEL/EXT-98-00964

Engineered Barrier Testing at the INEEL Engineered Barriers Test Facility: FY-1997 and FY-1998

Indrek Porro
Karen N. Keck

Published September 1998

Idaho National Engineering and Environmental Laboratory
RWMC Operations Department
Lockheed Martin Idaho Technologies Company
Idaho Falls, Idaho 83415

Prepared for the
U.S. Department of Energy
Assistant Secretary for Environmental Management
Under DOE Idaho Operations Office
Contract DE-AC07-94ID13223

SUMMARY

Engineered barriers of two designs are being tested at the Engineered Barriers Test Facility (EBTF) at the Idaho National Engineering and Environmental Laboratory. This report describes the test facility, barrier designs, and instruments used to monitor the test plots. Wetting tests conducted on the test plots in FY-97 are described and data collected from monitoring the test plots before, during and after the wetting tests are used to evaluate the performance of the covers during FY-97 and FY-98.

The EBTF is a concrete structure consisting of five cells (plots) on either side of an enclosed access trench. The access trench serves primarily as a protected area for the data acquisition system. Each cell measures 3 m wide by 3 m long by 3 m deep and is open to the atmosphere. Each cell has two floor drains that empty into separate sumps in the access trench. One drains a 10-cm wide trough along the inside perimeter of the cell. The other drains the remaining central portion of the cell.

Replicates of two engineered barrier designs were constructed in the EBTF cells. The first design comprises a thick, vegetated soil cover. The second design incorporates a capillary/biobarrier within the vegetated soil cover. The capillary barrier uses the textural break between an upper, fine textured soil and a lower, coarser-textured gravel layer to inhibit drainage under unsaturated conditions while increasing soil moisture storage in the root zone. Evaporation and transpiration by plants (although the test plots have not yet been vegetated) are used to recycle water stored in the soil back to the atmosphere. A geotextile fabric is used to maintain separation of the soil and gravel layers. A thick layer of cobbles beneath the gravel layer serves as a biobarrier to prevent intrusion of plant roots and burrowing animals into underlying waste (there is no waste in the test plots).

Each test plot was instrumented with time domain reflectometry probes and neutron probe access tubes to measure moisture contents, tensiometers, heat dissipation sensors, and thermocouple psychrometers to measure matric potentials, thermocouples to measure soil temperature, and ion-exchange resin beads to monitor tracer movement. Each drainage sump is equipped with a tipping bucket instrument and pressure transducer to measure drainage. Precipitation is measured using a heated rain gauge located at the EBTF. Instrument calibration equations and equation coefficients are presented, and data reduction techniques are described.

After their construction in the spring of 1996, the test plots were subject to ambient conditions at the EBTF. Prior to the wetting tests, differences in water distribution within the test plots were observed between the two cover designs. Water from precipitation had infiltrated deeper in the thick soil test plots than in the capillary/biobarrier test plots where the capillary barrier halted its downward progression. In spite of the infiltration, no drainage was observed in any of the test plots.

The wetting tests were designed to stress the test plots to the maximum by forcing drainage to occur. Drainage generally occurred two to three days following the start of the wetting test. Drainage from the capillary/biobarrier test plots stopped sooner than drainage from the thick soil test plots. Similar results were observed in drainage data collected in FY-98 following the spring thaw. Drainage from the capillary/biobarrier test plots following the winter of 1998 represents about one-third of the precipitation occurring during that period compared to two-thirds of the precipitation from the thick soil test plots. By limiting drainage, the capillary/biobarriers increased water storage in the upper portions of the test plots compared to the thick soil barriers. This led to increased recycling of water to the atmosphere through evaporation. Average evaporation from the capillary/biobarrier test plots was 21.65 cm and 16.21 cm in FY-97 and FY-98, respectively, compared to 10.39 cm and 6.12 cm from the thick soil test plots. Without

vegetation on the test plots to help recycle stored water back to the atmosphere, however, all test plots showed gradual gains in water storage during FY-97 and FY-98. The wetting tests also caused subsidence in all test plots. Subsidence was significantly greater (16.35 cm) in the thick soil test plots than in the capillary/biobarrier test plots (7.3 cm).

The data evaluated in this report come from an ongoing project. The aftereffects of the wetting tests continue to be monitored. Long-term monitoring under ambient conditions, the application of additional treatments to the test plots, and numerical modeling are planned for the future.

CONTENTS

FIGURES

TABLES

ACRONYMS

CFA	Central Facilities Area
EBTF	Engineered Barriers Test Facility
FY	Fiscal Year (October through September)
INEEL	Idaho National Engineering and Environmental Laboratory
PC	personal computer
PCT	plot cable tower
PVC	polyvinyl chloride
RWMC	Radioactive Waste Management Complex
SDA	Subsurface Disposal Area
TDR	time domain reflectometry

Engineered Barrier Testing at the INEEL Engineered Barriers Test Facility: FY-1997 and FY-1998

1. INTRODUCTION

Low-level radioactive waste is being disposed of at the Subsurface Disposal Area (SDA) of the Radioactive Waste Management Complex (RWMC) at the Idaho National Engineering and Environmental Laboratory (INEEL). Department of Energy Order 5820.2A requires a performance assessment of existing low-level waste facilities be conducted and that a closure/post-closure plan be written prior to closure of the facility. The closure plan for the facility must include a design for a closure cover. The current performance assessment of the SDA (Maheras, et al., 1994) assumes the presence of a closure cover that is effective in limiting net infiltration to 1 cm/yr. However, site-specific, field-validated data confirming the performance of specific cover designs do not exist. The need for such data is evident in view of the potentially significant impacts of the cover on facility performance and on meeting regulatory requirements.

Five engineered barrier designs were identified and evaluated (Keck, 1992) to determine which design(s) best met the performance objectives for the SDA closure cover. The alternatives considered were:

1) an evapotranspiration-storage cover with a capillary/biobarrier,

2) a thin soil-only evapotranspiration-storage cover,

3) a thick soil-only evapotranspiration-storage cover,

4) a Resource Conservation and Recovery Act three-layer cover, and

5) a concrete sealed surface cover.

Hydrologic performance analyses were conducted using numerical modeling as part of the evaluation. The analyses indicated that additional, site-specific data are needed to further characterize model input parameters, calibrate the models, and fully evaluate design alternatives. This evaluation led to the selection of two of the five cover designs for long-term field testing to provide the needed data. Design 1, an evapotranspiration-storage cover with a capillary/biobarrier, and design 3, a thick soil-only evapotranspiration-storage cover, were the two designs chosen for field testing.

The Engineered Barriers Test Facility (EBTF) was constructed for the purpose of field testing the cover designs. Test plots representing the two cover designs chosen for testing were established at the EBTF in the spring of 1996. Test plot construction and initial data gathered from monitoring the test plots are described by Porro and Keck (1997). The current report provides descriptions of: (1) the EBTF, (2) the instrumentation and measurement techniques used at the facility, (3) the data reduction methods, (4) the water balance components for the test plots from data collected from the facility in FY-1997 and FY-1998 (FY extends from October through September), and (5) future testing plans. The water balance analysis provides a comprehensive method with which to quantitatively analyze the performance of the engineered barriers. Accordingly, it is the focus of this report. Included in the Appendix to this report are summary tables of laboratory test results of soil physical and hydraulic properties of soil samples collected during

construction of the test plots (D.B. Stephens & Associates, Inc., 1997a and 1997b). These results are intended to document initial properties of the engineered barriers and serve as input to future modeling efforts.

2. DESCRIPTION OF THE FACILITY

2.1 Location

The EBTF is located near the RWMC in the southwestern corner of the INEEL (Figure 1). The EBTF is outside the RWMC fence to the north of the SDA in a disturbed area, used previously by U.S. Geological Survey personnel for weighing lysimeter studies. The proximity of the EBTF to the low-level waste disposal area at the SDA enhances the opportunity for testing the barriers under site-specific conditions.

2.2 Description of EBTF

The EBTF is a concrete structure consisting of five cells (plots) on either side of an enclosed access trench. Structural calculations and construction specifications for the EBTF may be found in Bragassa 1994 and 1995. Each cell has four walls and a floor and measures 3 m wide by 3 m long by 3 m deep. The top of each cell is open to the atmosphere. Because of shallow soil at this location, soil is bermed up around the facility so that cell tops are at grade level. Each cell has two floor drains that empty into separate sumps in the access trench. One drain drains a 10-cm wide trough that runs around the perimeter of the cell. The other drain drains the remaining central portion of the cell. Each drained area is sloped toward its drain. An additional opening in the floor of each cell provides a pathway for routing instrument cables from the cell to the access trench. Penetrations in the walls between the cells and the access trench provide direct access to some instruments.

The access trench is approximately 26.2 m long by 3.0 m wide by 3.8 m deep and serves primarily as a protected area for the data acquisition system and those instruments (tensiometers and resin capsule tubes) that penetrate the cell walls. A two-level Uni-Strut structure constructed in the trench is used to mount all the equipment enclosures for the data acquisition system. Instrument cables are routed in overhead cable raceways and along the Uni-Strut structure. A separate room at the south end of the access trench houses the data acquisition computer and serves as an office area.

The access trench is supplied with 115-V electrical service and a telephone line. A heat pump mounted on the south end of the roof of the access trench minimizes temperature variations and prevents freezing within the access trench.

2.3 Description of Test Plots

Figure 2 illustrates the two engineered barrier designs being tested at the EBTF. Four replicates of each design were built. Two test plots of each design will be subjected to natural meteorological conditions. One test plot of each design will be subjected to supplemental (2 x normal) precipitation. One test plot of each design will be subjected to two design storm events (a 25-yr, 24-hr storm, and a 100-yr, 24-hr storm). Two additional test plots were built with the thick soil barrier design. One of these plots will be used for in-situ hydraulic testing of the Spreading Area B cover soil. The other plot will be subject to destructive sampling and will provide additional samples for laboratory determination of hydraulic and physical properties of the cover soil. Figure 3 illustrates the layout of the test plots. More detailed design specifications for the two engineered barriers are presented by Eastman et al. (1992).

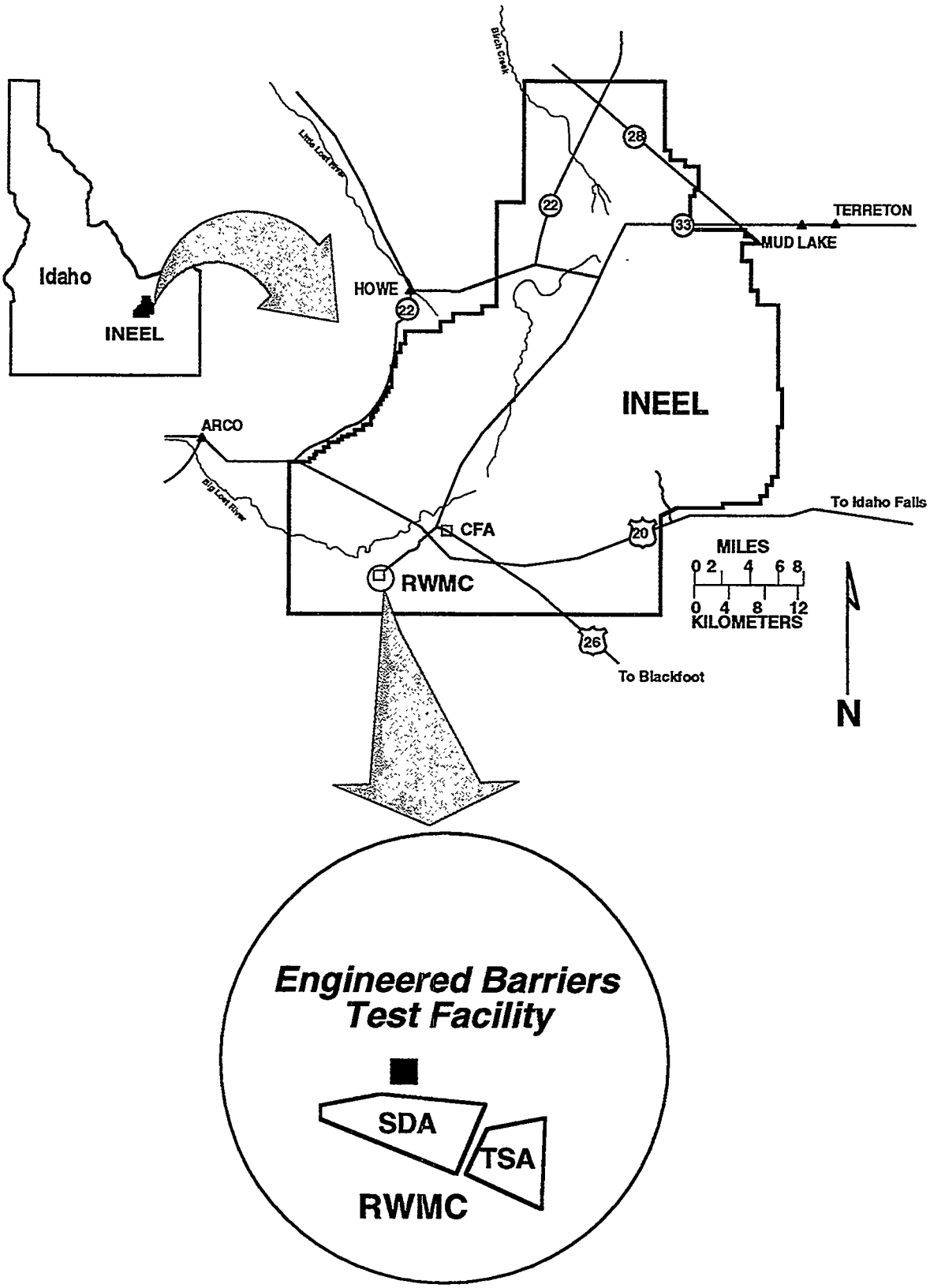

Figure 1. Site of the Engineered Barriers Test Facility at the INEEL.

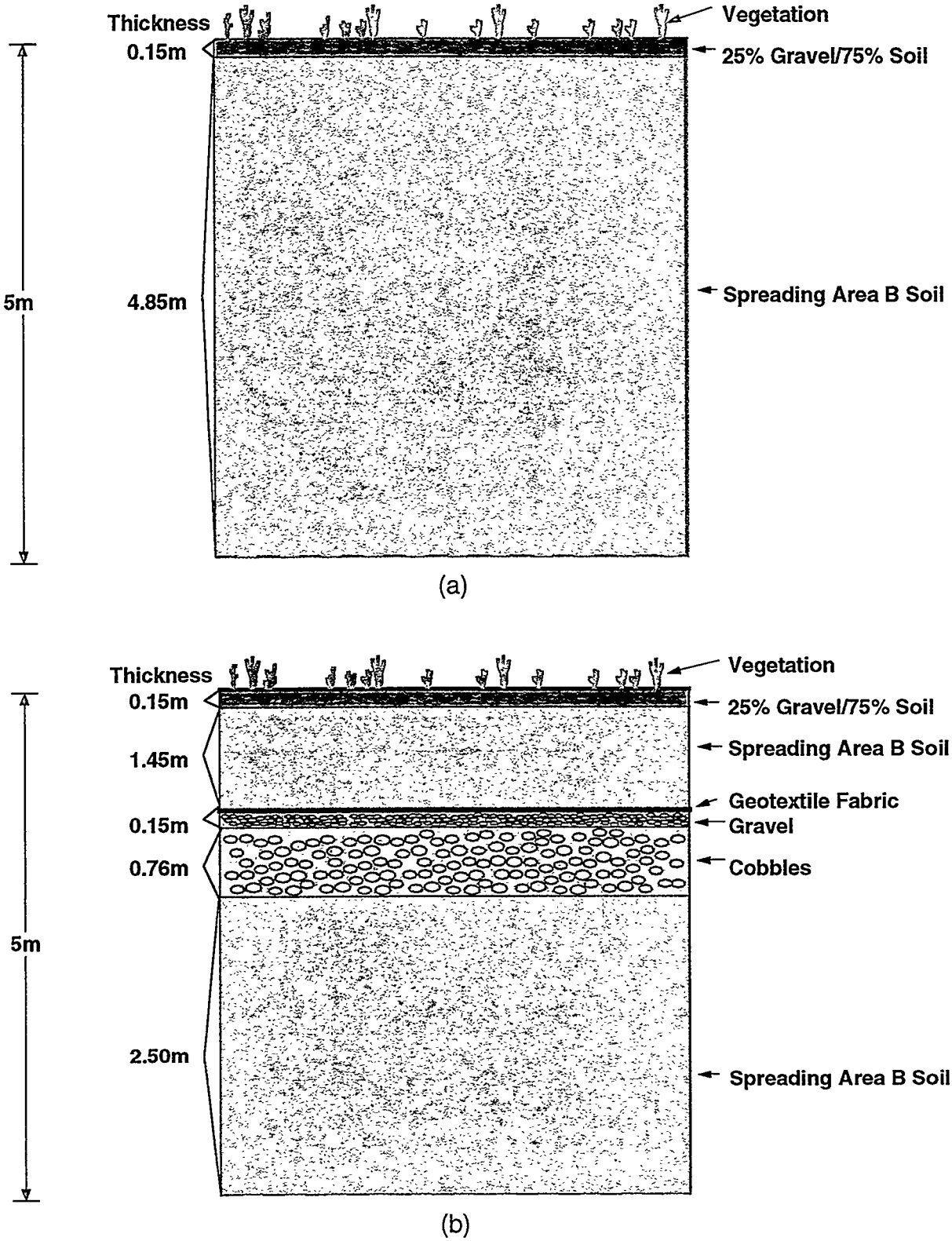

Figure 2. Schematic of the cover design (a) consisting of a thick soil and (b) incorporating a capillary/biobarrier.

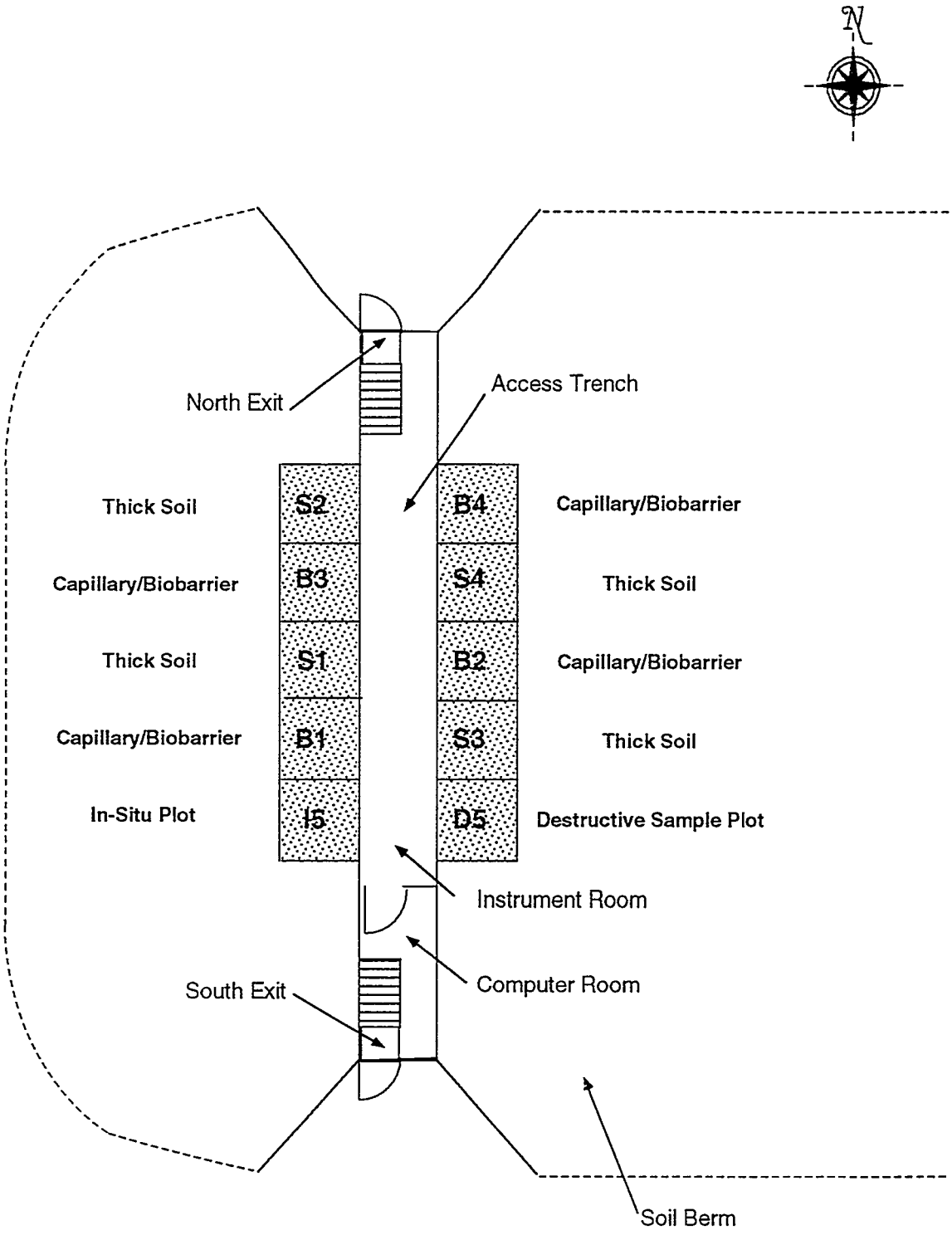

Figure 3. Layout of test plots at the EBTF.

3. INSTRUMENTATION AND MEASUREMENT TECHNIQUES

Drainage from each test plot is measured in two ways: (1) with a tipping bucket device and (2) with a pressure transducer. The tipping bucket device is attached to the drain pipe entering the sump. It serves to measure small flows (it registers one tip per 4.75 ml of water) from the test plot. The pressure transducer rests on the floor of the sump and is used to measure the level of water accumulations in the sump. Readings from both types of instruments are made automatically by the EBTF data acquisition system. Details regarding all instrument types, the data acquisition system, and system configuration are provided by Kaser and Adler Flitton (1997). Operating procedures for all instruments and proper data collection may be found in Porro and Keck 1996.

Soil moisture content is measured with time domain reflectometry (TDR) and neutron probe instrumentation. The TDR probes are buried in the test plots and are read automatically by the data acquisition system. The neutron probe access tubes are installed vertically in each test plot and measurements are made manually. Table 1 and Figure 4 show the areal positions and the depths of the instruments.

Soil matric potential is measured using tensiometers, heat dissipation sensors and thermocouple psychrometers. All of these instruments are buried in the test plots (see Table 1 and Figure 4). The tensiometers are equipped with pressure transducers for automatic data acquisition. Tensiometers will function in saturated conditions and in unsaturated conditions to matric potentials of -0.8 bar. The tensiometer pressure transducers, however, were calibrated in the range 1.034 to -1.034 bars. Heat dissipation sensors and thermocouple psychrometers were calibrated in the ranges -0.5 to -10 bars and -5 to -25 bars, respectively (D.B. Stephens & Associates, Inc., 1996). All heat dissipation sensors and thermocouple psychrometers are read automatically by the data acquisition system. Soil temperature is measured using thermocouples buried in the test plots (see Table 1 and Figure 4).

Ion exchange resin capsules will be used to monitor soil water tracer movement in the test plots. Resin capsule access tubes were installed in each test plot (see Table 1 and Figure 4). These access tubes were installed horizontally through penetrations in the access trench wall. Resin capsules will be installed manually through these access tubes after a tracer is applied at the soil surface. At periodic intervals, they will be manually removed and sent to a laboratory for chemical analysis of the tracer.

Precipitation at the EBTF is measured using a tipping bucket rain gauge equipped with a heater. This rain gauge is located on the surface of the berm surrounding the test plots. The rain gauge is read automatically by the data acquisition system.

Cables from all instruments buried in a test plot were routed to a plot cable tower (PCT). Each PCT is centrally located within a plot and serves to minimize cable intrusions within the plot as well as provide a centralized path for cables exiting the plot. The PCT is installed vertically within the plot and does not extend to the plot surface, thereby minimizing surface penetrations and possible artificially created pathways for water flow into the plot.

Table 1. Locations of EBTF instruments.

Instrument	Position	Depth (cm)
TDR	02,06,12	20,40,60,80,100,120,140,155,(180)[a],(205),(230),255,295
Neutron Probe	04,08	—
Tensiometer	03,10	40,60,80,100,120,140,[155][b],(180),255,295
Thermocouple Psychrometer	08,12	20,60,100,155,(205),255,295
Heat Dissipation Sensor	02,04	20,60,100,155,(205),255,295
Thermocouple	05,07	5,20,40,60,80,155,270
	01,03,06,10,13	60,270
Resin Capsule	09,11	80,155,255,295

a. Parentheses denote depths in thick soil barrier test plots only.

b. Brackets denote depths in capillary/biobarrier test plots only.

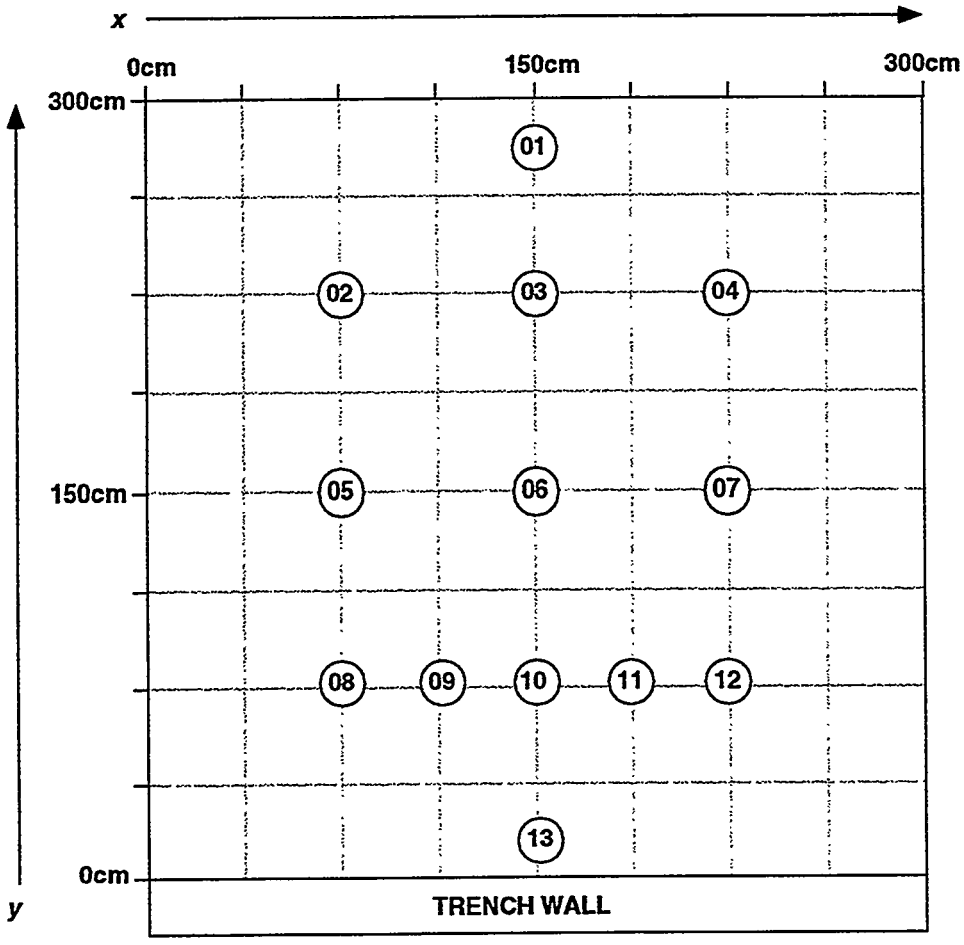

Figure 4. Plan view of a typical EBTF test plot showing instrument positions.

4. DATA ACQUISITION AND REDUCTION

Data from all instruments (except the neutron probe and resin capsules) are collected automatically using dataloggers. All dataloggers are linked to a central personal computer (PC) located at the south end of the access trench. End-to-end modems provide remote access to the central computer from the principal project scientist's office in Idaho Falls, Idaho. Detailed descriptions of the data acquisitions system including instrumentation, the instrument numbering system, datalogging equipment, system layout, datalogger program instruction sets, electrical wire configuration drawings, instrument configuration tables, recalibration schedules, acquired data file content descriptions, and instrument uncertainty analyses are presented by Kaser and Adler Flitton (1997). Acquired data files are stored on redundant personal computer data storage devices. Data reduction and analyses are currently being done using PC spreadsheet software. The following subsections describe the instrument calibration equations used to translate raw data in the acquired data files to appropriate soil parameters.

4.1 TDR

The TDR dataloggers are programmed to record the square root of the apparent dielectric constant, K_a, from each TDR probe. The volumetric soil moisture content (θ_v) is determined using the equation presented by Topp et al. (1980):

$$\theta_v(m^3/m^3) = 4.3\times10^{-6}K_a^3 - 5.5\times10^{-4}K_a^2 + 2.92\times10^{-2}K_a - 5.3\times10^{-2}. \quad (1)$$

4.2 Thermocouple Psychrometers

The thermocouple psychrometer dataloggers are programmed to record the temperature-corrected voltage from each thermocouple psychrometer. The matric potential (ψ) is determined using the equation

$$\psi(-bars) = A \times Temperature\ Corrected\ Voltage\ (\mu V) - B \quad (2)$$

where A and B are empirically determined coefficients. The thermocouple psychrometers were calibrated using several different molar solutions of sodium chloride (D.B. Stephens & Associates, Inc., 1996). EBT instrument IDs and calibration laboratory IDs for the thermocouple psychrometers are reconciled in Table 2, which also contains the calibration equation coefficients.

4.3 Heat Dissipation Sensors

The heat dissipation sensor dataloggers are programmed to record the temperature differential from each heat dissipation sensor. The matric potential (ψ) is determined using the equation

$$\psi(-bars) = A \times Temperature\ Differential\ (^\circ C)^B \quad (3)$$

where A and B are empirically determined coefficients. The heat dissipation sensors were calibrated using pressure pot extractors (D.B. Stephens & Associates, Inc., 1996). EBT instrument IDs and calibration laboratory IDs for the heat dissipation sensors are reconciled in Table 3, which also contains the calibration equation coefficients.

Table 2. Thermocouple psychrometer IDs and calibration equation coefficients.

Instrument ID	Laboratory ID	Coefficient A	Coefficient B
B1TP08020	35666	2.2574	0.5034
B1TP12020	35672	2.4860	-0.3015
B1TP08060	35662	2.6644	-1.0291
B1TP12060	35670	2.2142	0.1555
B1TP08100	35653	2.2047	0.9428
B1TP12100	35641	2.3514	-0.4596
B1TP08155	35660	2.2570	0.3524
B1TP12155	35655	2.2448	0.4427
B1TP08255	35644	2.4986	1.0398
B1TP12255	35658	2.3103	0.8257
B1TP08295	35648	2.2402	0.5461
B1TP12295	35663	2.2200	0.1388
B2TP03020	35706	2.2616	0.8622
B2TP10020	35688	2.2917	0.3031
B2TP08060	35710	2.2106	0.9073
B2TP12060	35683	2.2950	-0.6875
B2TP08100	35687	2.2576	0.9406
B2TP12100	35699	2.5129	1.7119
B2TP08155	35679	2.2765	0.8048
B2TP12155	35678	2.3515	0.2422
B2TP08255	35676	2.2644	0.8580
B2TP12255	35707	2.1985	0.3238
B2TP08295	35684	2.4903	-0.7434
B2TP12295	35720	2.1865	0.7070
B3TP03020	35652	2.1872	-0.1514
B3TP10020	35632	2.1881	-0.1812
B3TP08060	35628	2.3325	-0.0901
B3TP12060	35659	2.2682	0.8890
B3TP08100	35650	2.2250	-0.7408
B3TP12100	35625	2.2173	0.4091
B3TP08155	35626	6.2881	2.5376
B3TP12155	35620	2.4657	1.2823
B3TP08255	35633	2.1891	0.4624
B3TP12255	35638	1.9365	-2.0810
B3TP08295	35675	2.6667	1.3143
B3TP12295	35637	2.1322	-1.3511
B4TP03020	35673	2.3494	-0.1686
B4TP10020	35636	2.3135	0.7362
B4TP08060	35667	2.2172	-0.0561
B4TP12060	35669	2.5370	-1.6600

Table 2. (continued).

Instrument ID	Laboratory ID	Coefficient A	Coefficient B
B4TP08100	35674	2.3063	0.7825
B4TP12100	35668	2.1208	-0.3718
B4TP08155	35634	2.1934	0.0146
B4TP12155	35661	2.2182	0.2682
B4TP08255	35664	2.3814	0.5667
B4TP12255	35671	2.2975	-0.3811
B4TP08295	35704	2.4648	1.1256
B4TP12295	35665	2.2794	-0.5559
S1TP03020	35703	2.3181	1.5904
S1TP10020	35694	2.5918	3.0711
S1TP08060	35711	2.5177	-2.4264
S1TP12060	35677	2.3664	-1.7191
S1TP08100	35635	2.2556	0.1712
S1TP12100	35698	2.4707	1.2633
S1TP08155	35642	2.3567	-2.0337
S1TP12155	35716	2.5237	1.2435
S1TP08205	35645	2.3408	0.3880
S1TP12205	35702	2.1984	0.6301
S1TP08255	35643	2.7349	-2.1789
S1TP12255	35646	2.3007	1.0707
S1TP08295	35695	2.1920	0.1068
S1TP12295	35647	2.2889	-0.5201
S2TP03020	35715	3.1247	4.6323
S2TP10020	35692	2.2219	0.7963
S2TP08060	35705	3.8919	-2.4665
S2TP12060	35640	2.1945	-0.4738
S2TP08100	35682	2.1793	1.0933
S2TP12100	35722	2.2474	1.2485
S2TP08155	35723	3.8482	2.6632
S2TP12155	35721	2.2501	1.3221
S2TP08205	35681	2.9200	-1.2360
S2TP12205	35685	3.5352	-2.9753
S2TP08255	35686	2.3215	0.3201
S2TP12255	35680	2.2062	0.0957
S2TP08295	35718	2.2214	0.4647
S2TP12295	35719	2.3080	1.1836
S3TP03020	35649	2.2142	0.5971
S3TP10020	35639	2.3124	-1.0067
S3TP08060	35657	2.1595	-0.0246
S3TP12060	35656	2.2967	0.5497
S3TP08100	35627	2.0786	-1.8059

Table 2. (continued).

Instrument ID	Laboratory ID	Coefficient A	Coefficient B
S3TP12100	35622	2.2659	0.9409
S3TP08155	35623	2.3551	1.1138
S3TP12155	35654	2.2047	0.8873
S3TP08205	35651	7.1511	2.9553
S3TP12205	35631	2.2109	0.8797
S3TP08255	35630	2.2241	0.9313
S3TP12255	35624	2.3005	0.9596
S3TP08295	35621	2.2231	0.6576
S3TP12295	35629	2.1295	-0.2728
S4TP03020	35717	2.2081	0.7651
S4TP10020	35689	2.6093	0.0824
S4TP08060	35709	2.2495	0.6650
S4TP12060	35708	2.2387	0.6742
S4TP08100	35712	2.2890	1.1697
S4TP12100	35714	2.2420	0.7545
S4TP08155	35690	2.3205	0.6205
S4TP12155	35691	2.7470	0.2952
S4TP08205	35700	2.2539	0.1484
S4TP12205	35693	2.2839	-0.8951
S4TP08255	35701	2.2135	0.9987
S4TP12255	35697	2.1698	-0.6330
S4TP08295	35696	2.4987	0.4413
S4TP12295	35713	2.3316	1.0418

Table 3. Heat dissipation sensor IDs and calibration equation coefficients.

Instrument ID	Laboratory ID	Coefficient A	Coefficient B
B1HD02020	1684	0.0404	4.7273
B1HD04020	1687	0.0389	4.6894
B1HD02060	1689	0.0662	4.3717
B1HD04060	1691	0.1177	4.1762
B1HD02100	1682	0.0055	5.6443
B1HD04100	1680	0.0088	5.8829
B1HD02155	1677	0.0059	6.1388
B1HD04155	1676	0.0147	5.1832
B1HD02255	1674	0.0015	7.6496
B1HD04255	1675	0.0434	4.9334
B1HD02295	1782	0.1953	4.0480
B1HD04295	1781	0.0806	4.6556
B2HD02020	1757	0.0671	5.5066
B2HD04020	1758	0.1296	4.7717
B2HD02060	1795	0.0413	5.0974
B2HD04060	1754	0.0487	5.5604
B2HD02100	1793	0.1440	4.5431
B2HD04100	1794	0.1249	4.4983
B2HD02155	1791	0.1268	5.0156
B2HD04155	1792	0.0916	4.8276
B2HD02255	1790	0.1509	4.2192
B2HD04255	1789	0.0963	4.6607
B2HD02295	1779	0.2040	3.5630
B2HD04295	1780	0.0205	6.1367
B3HD02020	1697	0.0689	4.2809
B3HD04020	1700	0.0094	5.4024
B3HD02060	1701	0.0035	4.6718
B3HD04060	1702	0.0259	4.6964
B3HD02100	1703	0.0920	4.3928
B3HD04100	1704	0.0189	5.0875
B3HD02155	1698	0.0588	4.5478
B3HD04155	1705	0.0414	4.5720
B3HD02255	1774	0.2980	3.3921
B3HD04255	1773	0.1243	3.7986
B3HD02295	1787	0.2165	3.9725
B3HD04295	1786	0.1044	5.0601
B4HD02020	1672	0.0138	6.3764
B4HD04020	1661	0.0314	4.9961
B4HD02060	1670	0.0375	5.1339

Table 3. (continued).

Instrument ID	Laboratory ID	Coefficient A	Coefficient B
B4HD04060	1679	0.0279	5.8360
B4HD02100	1688	0.0563	4.3801
B4HD04100	1686	0.0105	5.1683
B4HD02155	1690	0.0346	4.9136
B4HD04155	1685	0.0517	4.4060
B4HD02255	1681	0.0801	4.0059
B4HD04255	1683	0.0483	4.5809
B4HD02295	1777	0.3147	3.3718
B4HD04295	1778	0.0602	4.9257
S1HD02020	1755	0.0904	4.5192
S1HD04020	1753	0.1658	4.2687
S1HD02060	1751	0.0918	4.6568
S1HD04060	1752	0.1536	4.4208
S1HD02100	1749	0.0143	6.0787
S1HD04100	1750	0.1091	4.6579
S1HD02155	1748	0.2655	3.6783
S1HD04155	1759	[a]	[a]
S1HD02205	1747	0.0168	5.6706
S1HD04205	1745	0.0810	4.8490
S1HD02255	1771	0.0528	5.2878
S1HD04255	1772	0.0796	4.9237
S1HD02295	1775	0.1248	4.6278
S1HD04295	1783	0.1459	3.7531
S2HD02020	1665	0.0504	4.3598
S2HD04020	1756	0.2047	4.0691
S2HD02060	1664	0.0336	4.8238
S2HD04060	1662	0.0548	5.1498
S2HD02100	1707	0.0400	4.4419
S2HD04100	1695	0.0295	5.2959
S2HD02155	1663	0.0126	5.4111
S2HD04155	1678	0.0120	5.9371
S2HD02205	1706	0.0860	4.1246
S2HD04205	1699	0.0795	4.0506
S2HD02255	1708	0.1186	4.2939
S2HD04255	1709	0.0987	4.3401
S2HD02295	1788	0.1400	3.9151
S2HD04295	1796	0.0527	4.7923
S3HD02020	1660	0.0215	5.3710
S3HD04020	1671	0.0166	5.6880
S3HD02060	1668	0.0163	5.4928
S3HD04060	1669	0.0377	4.7066

Table 3. (continued).

Instrument ID	Laboratory ID	Coefficient A	Coefficient B
S3HD02100	1666	0.0751	4.6257
S3HD04100	1667	0.0162	5.4280
S3HD02155	1692	0.0749	4.3681
S3HD04155	1693	0.0181	5.1759
S3HD02205	1694	0.0205	5.2959
S3HD04205	1696	0.0444	4.5233
S3HD02255	1746	0.0826	4.8623
S3HD04255	1744	0.1951	4.1093
S3HD02295	1784	0.2198	3.5078
S3HD04295	1785	0.3801	3.2225
S4HD02020	1770	0.1597	4.5580
S4HD04020	1743	0.0001	13.9020
S4HD02060	1766	0.1090	4.6505
S4HD04060	1769	0.0780	4.9076
S4HD02100	1767	0.0643	5.1277
S4HD04100	1768	0.0280	5.8677
S4HD02155	1764	0.2716	4.5262
S4HD04155	1765	0.0234	5.3463
S4HD02205	1762	0.0147	6.2821
S4HD04205	1763	0.1401	4.6707
S4HD02255	1760	0.0342	6.1439
S4HD04255	1761	0.1191	4.7510
S4HD02295	1776	0.2327	3.6837
S4HD04295	1673	0.0247	5.2036

a. Defective probe

4.4 Tensiometers

The tensiometer dataloggers are programmed to record the voltage from each tensiometer pressure transducer. The tensiometer pressure transducers were calibrated by applying different pressures (P) to the transducers and taking corresponding voltage readings. Pressure (0 to -15 psi) is linearly related to voltage (0 to -100 mV). Matric potential is calculated as follows:

$$\psi(bars) = Voltage(mV) \times \frac{-15\ psi}{-100\ mV} \times \frac{1\ bar}{14.504\ psi}. \quad (4)$$

4.5 Thermocouples

The thermocouple dataloggers are programmed to record the temperature (°C) from each thermocouple. No further reduction of this data is required.

4.6 Sump Tipping Bucket Devices

The sump tipping bucket datalogger is programmed to record the number of tipping bucket tips from each device. The sump tipping bucket devices are calibrated to measure 4.75 ml of water per tip. The amount of drainage (D) is determined using the equation

$$D(cm) = \frac{Tips \times 4.75}{Area(cm^2)} \tag{5}$$

where Area = 78,221 cm^2 for the center drain and Area = 11,779 cm^2 for the perimeter drain.

4.7 Sump Level Transducers

The sump level dataloggers are programmed to record the voltage from each sump level pressure transducer. The sump level pressure transducers were calibrated by applying different pressures (P) to the transducers and taking corresponding voltage readings. The pressure and voltage readings are linearly related:

$$P(psi) = A + B \times Voltage(mV) \tag{6}$$

where A and B are empirically determined coefficients. Pressure is then converted to an equivalent depth of water (D) on a plot area basis using

$$D(cm) = \frac{P(psi) \times 281{,}786}{Area(cm^2)} \tag{7}$$

where Area = 78,221 cm^2 for the center drains and Area = 11,779 cm^2 for the perimeter drains. The area of each sump is 4,008.06 cm^2.

EBT instrument IDs and calibration laboratory IDs for the sump level pressure transducers are reconciled in Table 4, which also contains the calibration equation coefficients.

4.8 Rain Gauge

The rain gauge datalogger is programmed to record the number of tipping bucket tips. The rain gauge is calibrated to measure 0.01 in. of precipitation per tip. The amount of precipitation (P) is determined using the equation

$$P(cm) = Tips \times 0.01 \times 2.54\,. \tag{8}$$

4.9 Neutron Probe

The neutron probe readings are made manually. The neutron probe readings are counts of thermalized neutrons and are converted to volumetric soil moisture content (θ_v) using the equation for disturbed SDA sediments presented by Bishop (1996):

$$\theta_v(m^3/m^3) = \frac{2.396 \times 10^{-3} \times Counts + 4.627}{100}. \quad (9)$$

Table 4. Pressure transducer IDs and calibration equation coefficients.

Instrument ID	Laboratory ID	Coefficient A	Coefficient B
B1SL0C300	713927	-0.017110	0.000204
B1SL0E300	713924	0.015255	0.000198
B2SL0C300	713925	-0.026000	0.000199
B2SL0E300	713918	-0.018880	0.000201
B3SL0C300	713919	-0.031120	0.000200
B3SL0E300	713910	-0.012100	0.000201
B4SL0C300	713916	-0.003910	0.000202
B4SL0E300	713911	-0.023680	0.000200
D5SL0C300	713917	-0.028170	0.000201
D5SL0E300	713923	-0.018480	0.000199
I5SL0C300	713921	0.111123	0.000175
I5SL0E300	713913	0.013477	0.000199
S1SL0C300	713909	0.001917	0.000200
S1SL0E300	713914	0.019609	0.000203
S2SL0C300	713922	0.003099	0.000199
S2SL0E300	713920	-0.003970	0.000198
S3SL0C300	713929	0.033386	0.000203
S3SL0E300	713926	-0.006030	0.000201
S4SL0C300	713912	-0.012100	0.000197
S4SL0E300	713915	-0.018250	0.000200

5. WATER BALANCE EVALUATION

The function of the engineered barriers being studied at the EBTF is to minimize the infiltration of water to the underlying waste and the subsequent transport of contaminants leached from this waste to the aquifer. Rather than providing just an impermeable barrier to stop downward water movement, these barriers are designed to rely on several natural, interactive processes to function effectively. Determining the engineered barrier's water balance was identified as an effective way to evaluate the barrier's overall performance (Keck, 1992, Porro, et al., 1996).

The water balance of the engineered barrier test plots quantitatively accounts for all water impacting the test plots. The water balance equation is represented as:

$$\Delta S = P + I - R - D - ET \tag{10}$$

where ΔS is the change in soil water storage, P is precipitation, I is irrigation, R is surface runoff, D is drainage, and ET is evapotranspiration. Changes in soil water storage in the following water balance evaluation are based on water contents as measured by TDR probes. Precipitation is measured by the EBTF rain gauge. Irrigation (in the form of the wetting test water applications) is measured by flow meters. Drainage is measured by both tipping buckets installed at the outlet of the plot drains (to measure volume of drainage) and pressure transducers installed on the floor of the drainage sumps (to measure water level in the sump). Surface runoff is zero because the test cell side walls extend above the surface of the test plots. Evapotranspiration is determined by rearranging Equation 10 and solving for ET with measured values substituted for all other components. During FY-97 and FY-98, the ET term represents evaporation only because all plot surfaces were kept cleared of vegetation, thereby eliminating transpiration by plants. The following subsections discuss the individual components of the water balance equation for FY-97 and FY-98.

5.1 Water Inputs

5.1.1 Precipitation

Cumulative precipitation measured at the EBTF during FY-97 and FY-98 is shown in Figure 5 along with the long-term average precipitation measured at the Central Facilities Area (CFA). CFA (11 km northeast of the EBTF) is the nearest location to the EBTF where meteorological data have been collected for a long time. Total precipitation for each of the past two years was close to the long-term average (22.5 cm) with FY-97 being slightly above (24.4 cm) the long-term average and FY-98 being slightly below (19.1 cm) the long-term average (data from the last three weeks of FY-98 are not covered in this report so that the schedule for publishing this report could be met). The patterns of precipitation for the two years, however, differed from the long-term average and from each other. In FY-97 precipitation in December and the first few days of January was significantly greater than the long-term average. This was followed by over four months of below-average precipitation, which brought the total back to normal. Another period of rainfall in August raised the level above normal where it remained until the end of FY-97. In FY-98 precipitation in November and December was less than the long-term average and the cumulative amount remained below average until May. Precipitation remained near normal throughout early summer but fell slightly below normal toward the end of FY-98.

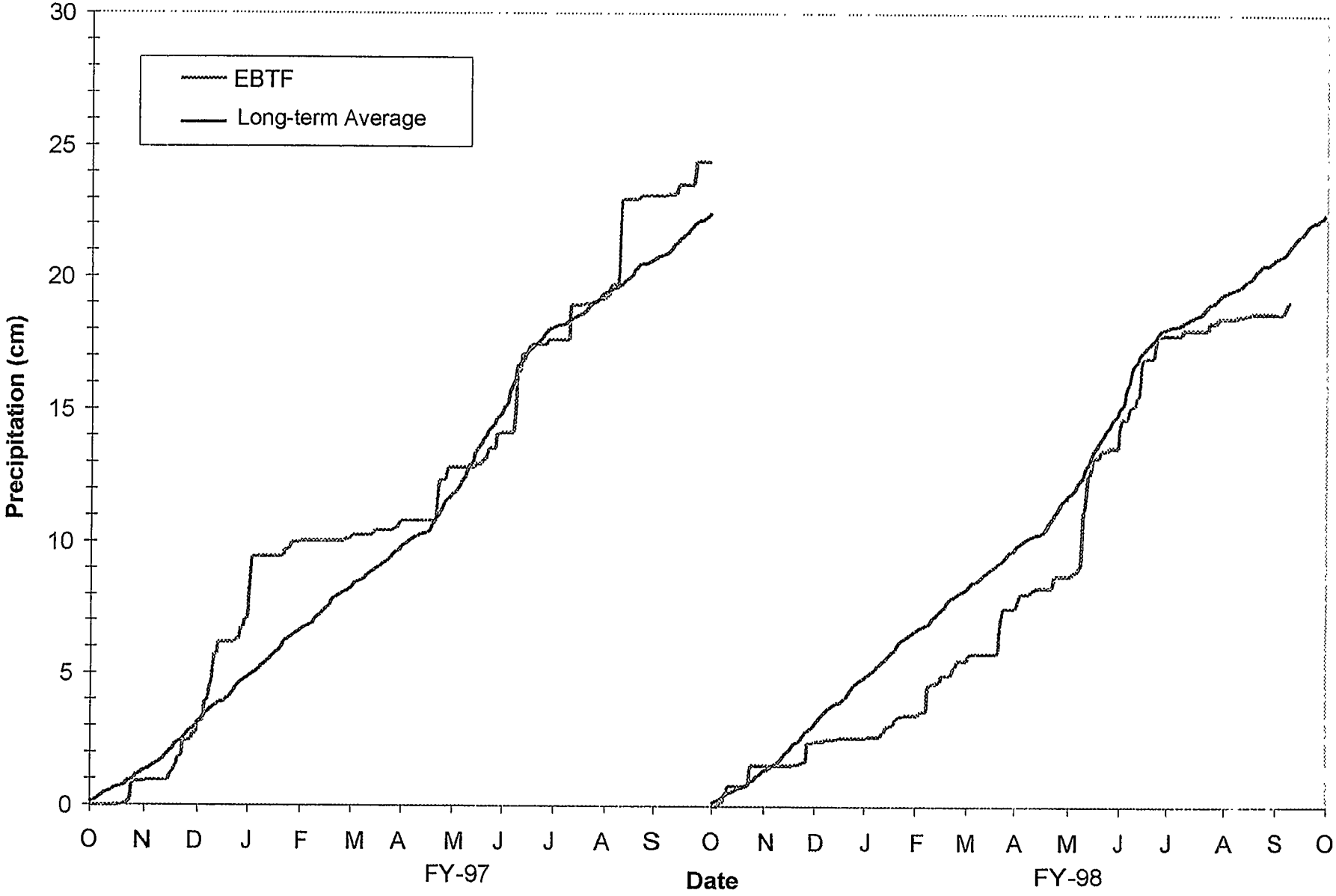

Figure 5. Cumulative precipitation at the EBTF during FY-97 and FY-98 and long-term average cumulative precipitation.

5.1.1.1 Snow. The long-term average precipitation at the INEEL is fairly uniform throughout the year, with the exception of late spring. The long-term average precipitation for May and June is 3.05 cm and 3.00 cm, respectively, compared to an average of 1.61 cm (with a range from 1.32 cm to 1.91 cm) for all other months. The temporal pattern of water infiltration (which may have a significant impact on the performance of an engineered barrier) resulting from precipitation, however, is more complex than the precipitation curve alone may indicate. Soil and air temperatures can have a significant impact on the amount and timing of infiltration due to precipitation. Precipitation with warm temperatures results in rainfall that can readily infiltrate into the soil. Precipitation in cold temperatures produces snow, which does not readily infiltrate into the soil. Infiltration resulting from snowfall can be delayed as long as the snow does not melt. Accumulating snow from numerous precipitation events can result in a significantly greater slug of infiltrating water when thawing occurs than individual precipitation events may indicate. Soil freezing can also prevent infiltration, thereby allowing water to accumulate prior to infiltration and decoupling the timing of infiltration and precipitation events.

Figure 6 shows cumulative snowfall measured at CFA during FY-97 and FY-98 and the long-term average snowfall. Daily snowfall is not measured at the EBTF. Snowfall in early December of FY-97 significantly exceeded the long-term average. However, by February the cumulative totals were equal. Total snowfall for FY-97 was less than normal. In FY-98 larger-than-normal snowfalls were distributed more evenly throughout the winter season. Cumulative snowfall exceeded the long-term average in early December and mid-January, but generally tracked the long-term average until February, when significant storms pushed the cumulative total beyond the long-term average.

Snow depths for FY-97, FY-98, and the long-term average snow depths are shown in Figure 7. In FY-97 snow covered the ground throughout December, but only sporadically before and after December. This is in contrast to the long-term average where snow covers the ground from November to April, with the greatest snow depth in late January. Snow covered the ground for a much longer time in FY-98. Spot checks of snow depths at the EBTF showed general agreement with levels recorded at CFA with one major exception. CFA reported complete disappearance of snow by March 1, 1998. On March 16, 1998 there were still several centimeters of snow at the EBTF. The snow was melting and there was standing water beneath the snow.

Blowing and drifting snow and human activities often redistribute snow on the landscape (and on engineered barriers). Consequently, it is of interest to know the water content (or water equivalent) of accumulated snow so that subsequent infiltration and/or runoff can be managed. A more general way of discussing the water equivalent is through the use of the term *snow density,* defined as the percentage of snow volume that would be occupied by its water equivalent. An estimate of the snow density can be made by calculating the ratio of daily precipitation (measured with a heated precipitation gauge) to the depth of daily snowfall. Daily precipitation and snowfall measured at CFA were used to calculate snow densities of 0.140 and 0.091 in FY-97 and FY-98, respectively, i.e., 100 cm of snow would be the equivalent of 14 cm of water in FY-97 and 9.1 cm of water in FY-98. It is highly likely that these numbers also would be characteristic of snow at the EBTF. The calculated values are snow densities of fresh-fallen snow. The density of snow on the ground generally increases over time due to gravitational settling, wind packing, melting, and recrystallization (Dunne and Leopold, 1978). The amount of increase depends on the intensity with which these factors operate and their interactions, and is difficult to calculate. Therefore, the depth of fresh snow may be an unreliable indicator of the snow density at some subsequent time.

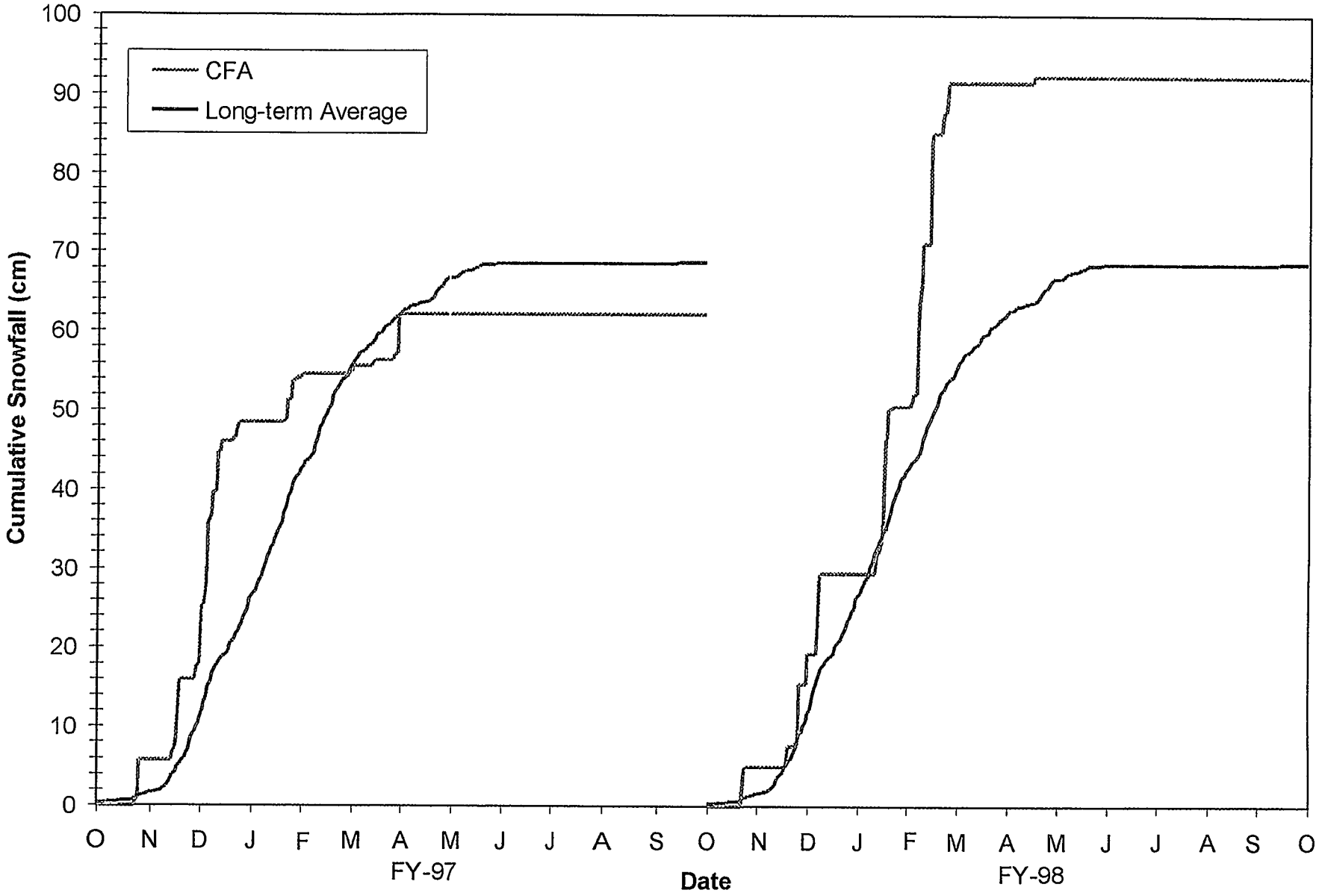

Figure 6. Cumulative snowfall at the EBTF during FY-97 and FY-98 and long-term average cumulative snowfall.

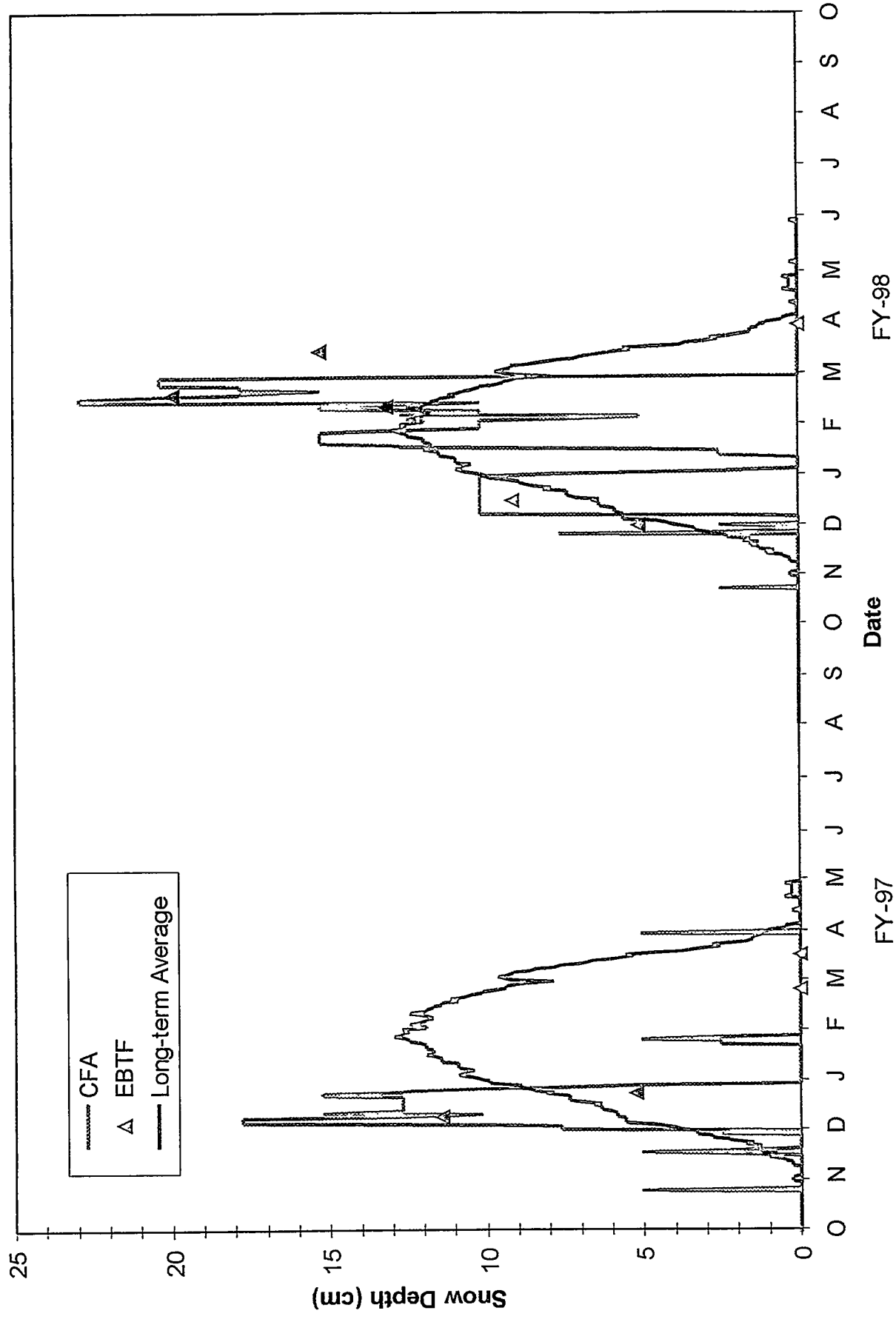

Figure 7. Snow depth at CFA and the EBTF during FY-97 and FY-98 and long-term average snow depth.

5.1.2 Wetting Tests

A wetting test was performed on all test plots during FY-97. Each wetting test consisted of applying water to the surface of the plot until drainage from the bottom of the plot began. This subsection describes the method of water application, the amount of water applied, and the subsidence that occurred during the wetting tests.

5.1.2.1. Applicators. Water was applied to each plot using a parallel array of soaker hoses attached to PVC pipe manifolds (Figure 8). These soaker hose arrays are referred to as applicators. Four applicators were built with each applicator sized to cover one test plot. A control system was devised to allow simultaneous, independent operation of four applicators. Water is delivered to the applicators by a pump that is controlled from a datalogger located in the access trench. A 1,200-gallon tank supplies water to the pump under gravity flow. Rate of flow is established using pulses of water produced by energizing the pump for specified lengths of time. Flows to one of four possible applicators are further controlled using in-line solenoid valves that are switched on for each pulse event. Both "on time" and "off time" can be varied in order to achieve the average flow rate desired. Monitoring of the applied volume of water is accomplished for each applicator using a paddle wheel flow meter that produces electric pulses that are captured by the datalogger. The datalogger can be programmed to provide either constant or varying application flow rates.

5.1.2.2. Water Applied. Wetting tests were conducted two plots at a time. One capillary/biobarrier test plot and its corresponding thick soil test plot were done simultaneously, i.e., plots B1 and S1, B2 and S2, B3 and S3, and B4 and S4. Supplemental test plots I5 and D5 were wetted individually. Water was applied to each plot by energizing the water supply pump for one minute every 15 minutes until drainage occurred. Water applications to that plot were then terminated. During water applications, scattered areas of shallow ponding were observed on plot surfaces. All ponded water infiltrated within 15 minutes, i.e., before the next pumping cycle. Cumulative amounts of water applied to each test plot are shown in Figure 9. Although wetting was initiated simultaneously on both capillary/biobarrier and thick soil test plots, the capillary/biobarrier test plots started draining first because water moved through the capillary/biobarrier (comprised of gravel and cobbles) more rapidly than through an equal depth of soil in the thick soil test plots. Turning off the water to the capillary/biobarrier test plot inadvertently increased flow to the thick soil test plot, hence the bimodal curves for the thick soil (S) test plots.

A power outage that occurred while wetting plot S4 terminated water application prior to initiation of drainage. Since moisture content measurements from within the plot indicated that the wetting front was close to the bottom of the plot at the time of the outage and that drainage was imminent, wetting was not reinitiated after the outage.

A solenoid failure during wetting of test plots B1 and S1 resulted in continuous water application to plot B1 after 17:00 hr on September 24, 1997. Water application stopped when the supply tank ran dry. As a result, test plot B1 received more water than plot S1. Drainage from plot B1 began during water application. Drainage from plot S1 had not started when the supply tank ran dry. Since freezing temperatures were predicted for the next few days and the application system is not designed for cold weather operation, the decision was made to terminate the wetting test.

Total amounts and rates of water applied to each test plot are shown in Table 5. The target rate of application for the wetting tests was 16.4 cm/day, based on an estimate of the soil's saturated hydraulic conductivity (Magnuson, 1993). Results from laboratory analyses (saturated hydraulic conductivity) of

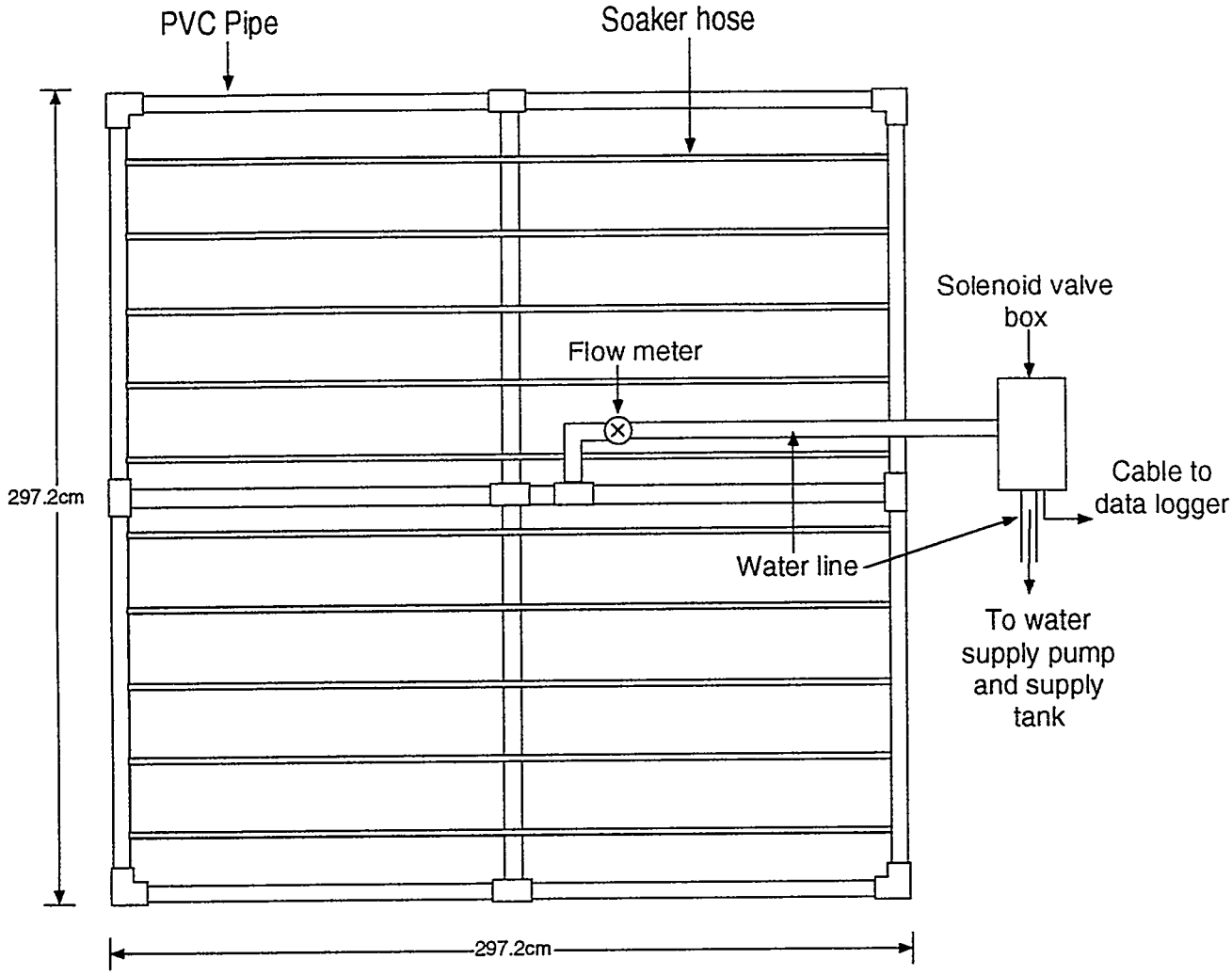

Figure 8. EBTF Irrigation Applicator.

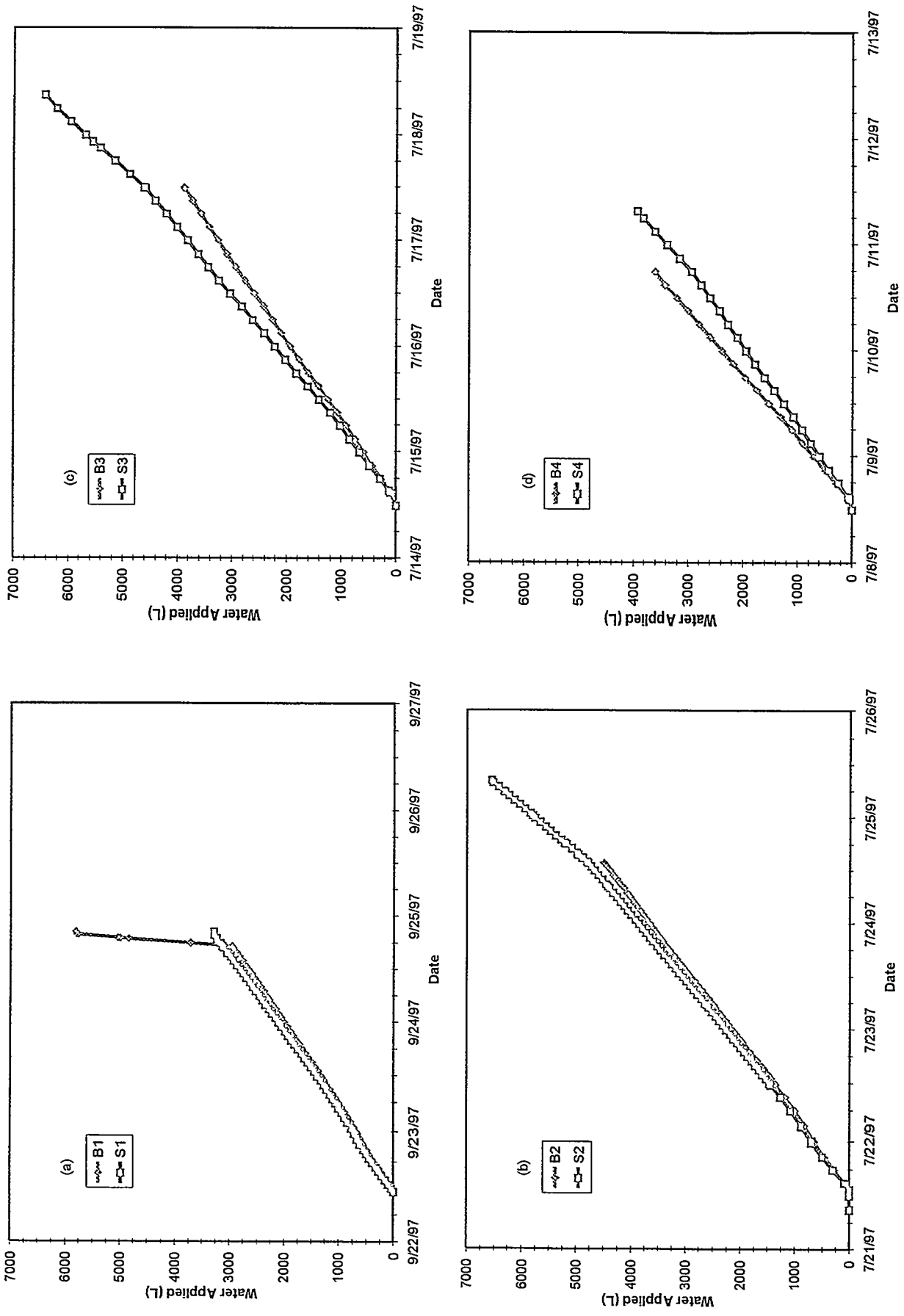

Figure 9. Water applied during FY-97 wetting tests.

Table 5. Dates and amounts of FY-97 wetting test water applications.

Plot	Water Application Period	Total Applied (L)	Total Applied (cm)	Time (d)	Rate Applied (cm/d)
B1	9-22-97 11:15 to 9-24-97 17:00	2,961	31.87	2.25	14.17
	9-24-97 17:00 to 9-24-97 20:32	2,854	30.72	0.14	219.43
S1	9-22-97 11:15 to 9-24-97 20:32	3,285	35.36	2.39	14.79
B2	7-21-97 9:00 to 7-24-97 13:50	4,499	48.43	3.20	15.13
S2	7-21-97 9:00 to 7-24-97 13:50	4,782	51.47	3.20	16.09
	7-24-97 13:50 to 7-25-97 8:26	1,768	19.03	0.78	24.40
B3	7-14-97 12:00 to 7-17-97 12:00	3,904	42.02	3.00	14.01
S3	7-14-97 12:00 to 7-17-97 12:00	4,619	49.72	3.00	16.57
	7-17-97 12:00 to 7-18-97 9:00	1,820	19.59	0.87	22.52
B4	7-8-97 12:00 to 7-10-97 18:00	3,624	39.01	2.25	17.34
S4	7-8-97 12:00 to 7-10-97 18:00	2,940	31.65	2.25	14.06
	7-10-97 18:00 to 7-11-97 7:37	996	10.72	0.57	18.81
D5	6-23-97 15:26 to 6-25-97 15:00	4,012	43.18	1.98	21.81
I5	7-29-97 11:00 to 7-30-97 11:00	2,164	23.29	1.00	23.29

soil samples taken during construction of the test plots were not available when the wetting tests were conducted.

5.1.2.3. Subsidence. All of the test plots subsided as a result of the wetting tests. Subsidence was measured at 25 locations on each plot using a 75-cm by 75-cm grid. A pipe was laid across each plot with its ends resting on the concrete edges of the plot to serve as a grid point locator and to establish a vertical reference point. Averages of the inner 3 by 3 grid subsidence measurements for each test plot are plotted in Figure 10. Measurements made along the outer edges of the plots are not included in the averages because subsidence along the edges appeared to be affected by the edges and not representative of overall plot subsidence.

Subsidence was significantly greater in the thick soil test plots than in the capillary/biobarrier test plots (Table 6). Thick soil test plots subsided an average of 16.35 cm whereas capillary/biobarrier test plots subsided an average of 7.3 cm. The amount of subsidence appears to be unrelated to the amount of water applied during the wetting tests. Wetting tests went as planned for plots B2 and S2 and plots B3 and S4, i.e., water was applied until drainage from the bottom was observed. Plots B2 and B3 required less water because water moved quickly through the 90-cm thick capillary/biobarrier zone causing earlier drainage than in S2 and S3. Plots B2 and B3 experienced less subsidence than plots S2 and S3. A power failure caused early termination of wetting for plot S4, i.e., water application stopped prior to observed drainage. Water application to plot B4 had already been terminated due to observed drainage. As a result of the power failure, plots B4 and S4 received comparable amounts of water during the test. Nevertheless, subsidence in plot S4 was still significantly greater than in B4. The solenoid failure during wetting of plots B1 and S1 resulted in application amounts that were the opposite of desired amounts, i.e., more water was applied to plot B1 than to plot S1. Although plot S1 received less water than plots B2, B3, and B4, it exhibited greater subsidence than those three B plots. Additionally, although plot B1 received more water than plots S4, D5, and I5, it exhibited less subsidence than those three thick soil plots. Finally, although supplemental test plot I5 received the least amount of water of any plot (water application was terminated intentionally prior to the onset of drainage), it showed significantly more subsidence than any of the capillary/biobarrier test plots.

Table 6. Analysis of variance results for testing differences in subsidence between cover designs.

Source of Variation	SS	df	MS	F	P-value
Between Designs	196.566	1	196.566	21.2921	0.001723
Within Designs	73.855	8	9.231875		
Total	270.421	9			

SS-Sum of Squares
df-degrees of freedom
MS-Mean of Squares

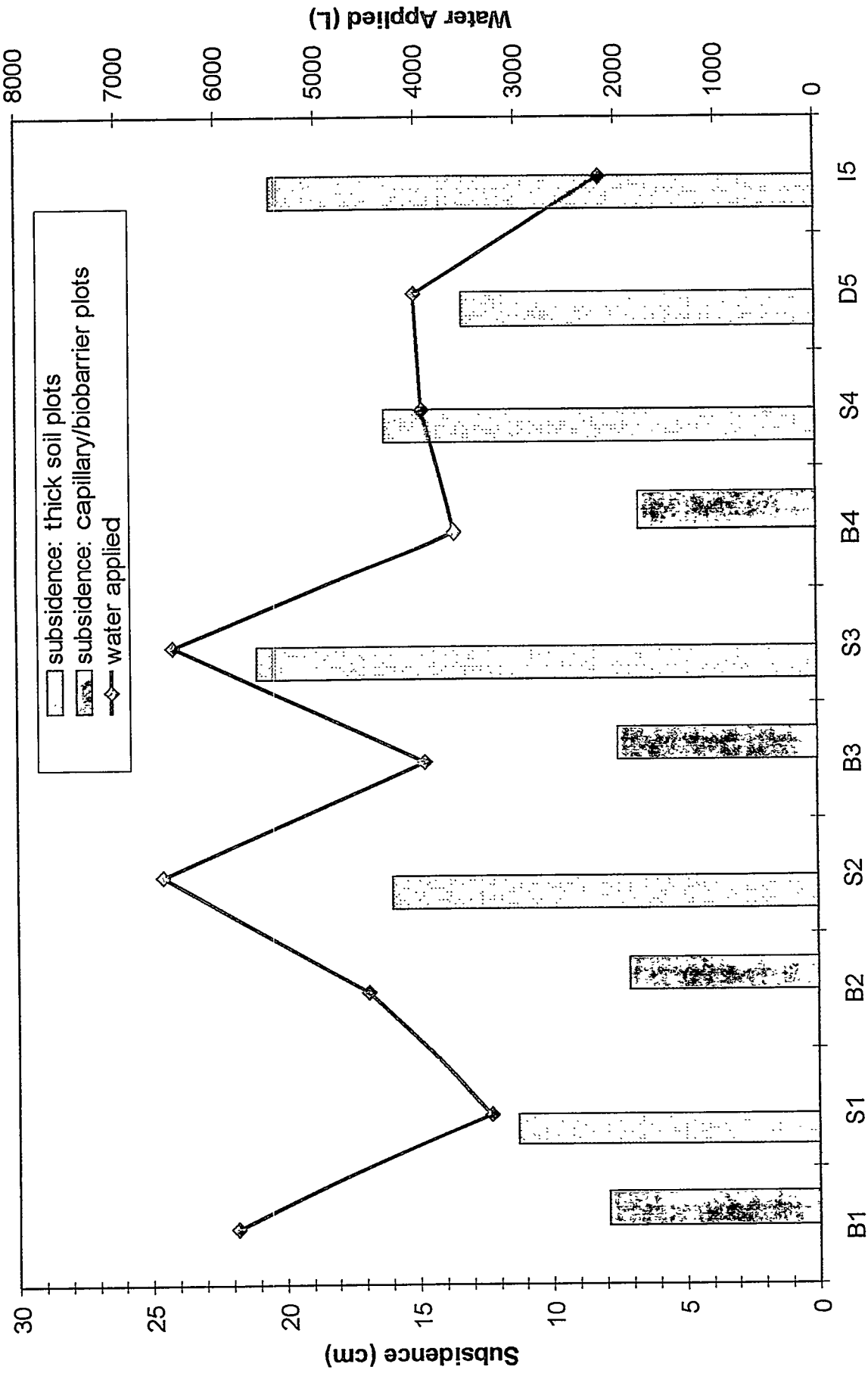

Figure 10. Depths of subsidence and amounts of water applied during FY-97 wetting tests.

5.2 Water Storage

Soil moisture contents were determined with the TDR probes hourly in FY-97 and once every three hours in FY-98. The amount of water stored in each test plot, S, was calculated as

$$S = \int_0^Z \theta \, dz \tag{11}$$

where Z is the depth of the test plot, θ is the volumetric water content, and z is the depth interval of the water content measurement.

Moisture contents in the 90-cm-thick capillary/biobarrier were not determined because TDR probes were not installed in that zone. This is of little consequence in the following discussion because the water holding capacity of the barrier zone is minimal.

Water storage as a function of time in all test plots is shown in Figure 11. The test plots were filled with air-dried soil and instrumented in the spring of 1996 (Porro and Keck, 1997). Consequently, water storage in the test plots at the start of FY-97 was low. Precipitation in November and December of 1996 and the first few days of January 1977 resulted in the first increases in water storage. Soil freezing, which presents a barrier to infiltration, was sporadic (see Figure 12), thus allowing the precipitation to infiltrate into the soil. The two-and-a-half month long depression in water storage following the early January infiltration is an artifact of the TDR probes which do not measure moisture content in the form of ice (see Porro and Keck, 1997). Figure 12 confirms the fact that the soils were frozen to at least the 60 cm depth from January to the latter half of March. Without transpiration from vegetation as a means of recycling water back to the atmosphere, water storage gradually increased as a result of infiltrating precipitation throughout the spring and early summer of 1997.

From a total water storage perspective, all of the test plots responded similarly during FY-97, i.e., there was essentially nothing to differentiate the capillary/biobarrier test plots from the thick soil test plots. However, water content profiles of the plots reveal that the internal distribution of water within the plots differed between the two designs. Figure 13 shows examples of water content profiles at position 12 in both types of test plots (specifically plots B2 and S2) on two dates, the latter profile comprised of data collected just prior to the start of the wetting tests. Water has clearly infiltrated to the 155 cm depth in plot B2 (Figure 13a). This is the position of the TDR probe closest to the top of the capillary/biobarrier (which begins at the 160 cm depth). Water content does not change at the 225 cm depth. This is the position of the TDR probe closest to the bottom of the capillary/biobarrier (which ends at the 250 cm depth). Although no TDR measurements are made within the capillary/biobarrier, it is reasonable to assume that under these unsaturated conditions the water content of this zone did not change and that the capillary barrier is effectively stopping downward water movement. In the absence of a capillary barrier, water infiltrated to the 230 cm depth during this same time in plot S2 (Figure 13b). No drainage was observed in any of the test plots prior to the wetting tests.

The most dominant feature of Figure 11 is the sharp rise in water storage during the summer of 1997. This rise represents the applications of water during the wetting tests. As discussed above, water was applied to the surface of the plots until drainage from the bottom of the plots was observed. The drainage continued even after the application of water ceased and is represented by decreasing water

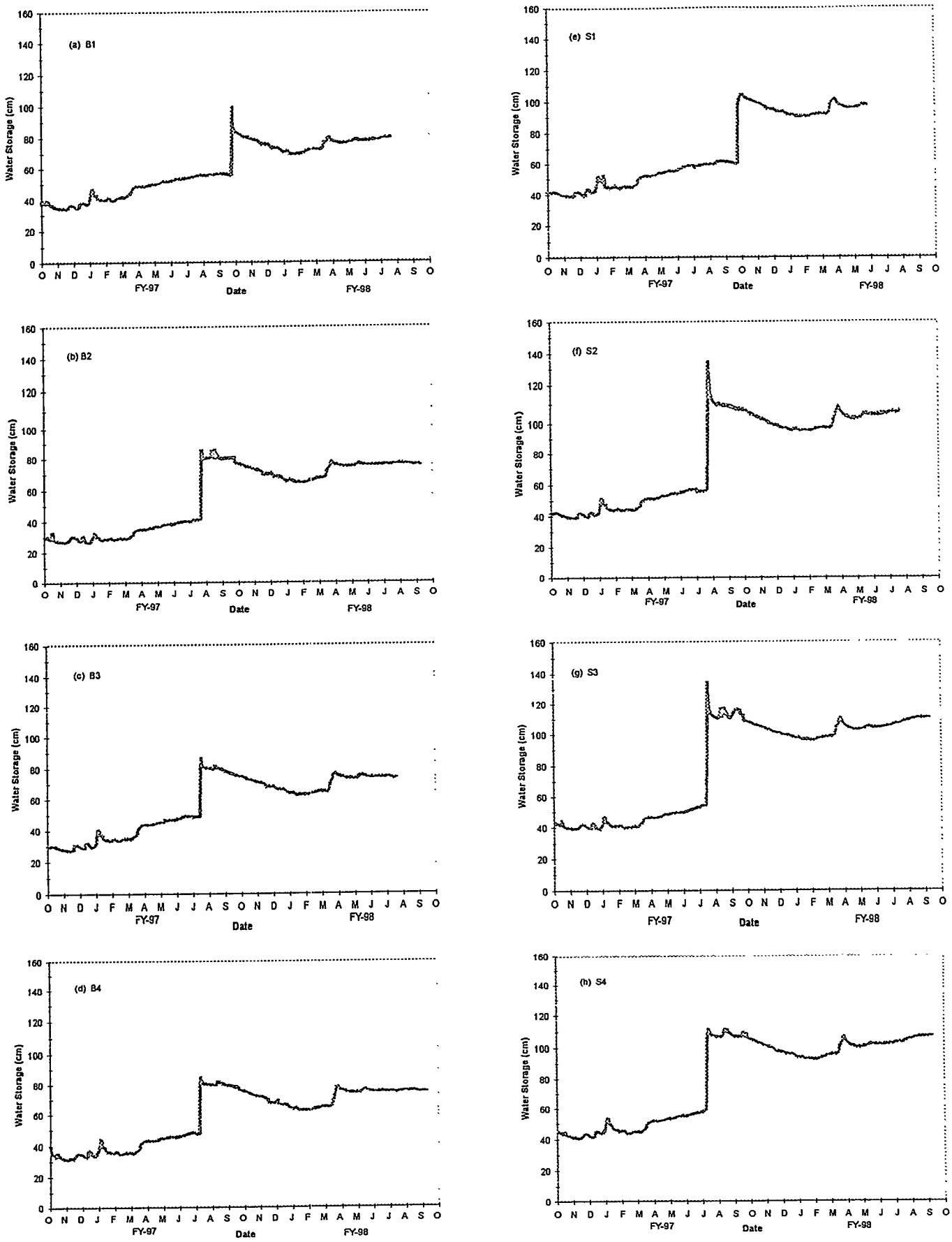

Figure 11. Soil water storage during FY-97 and FY-98.

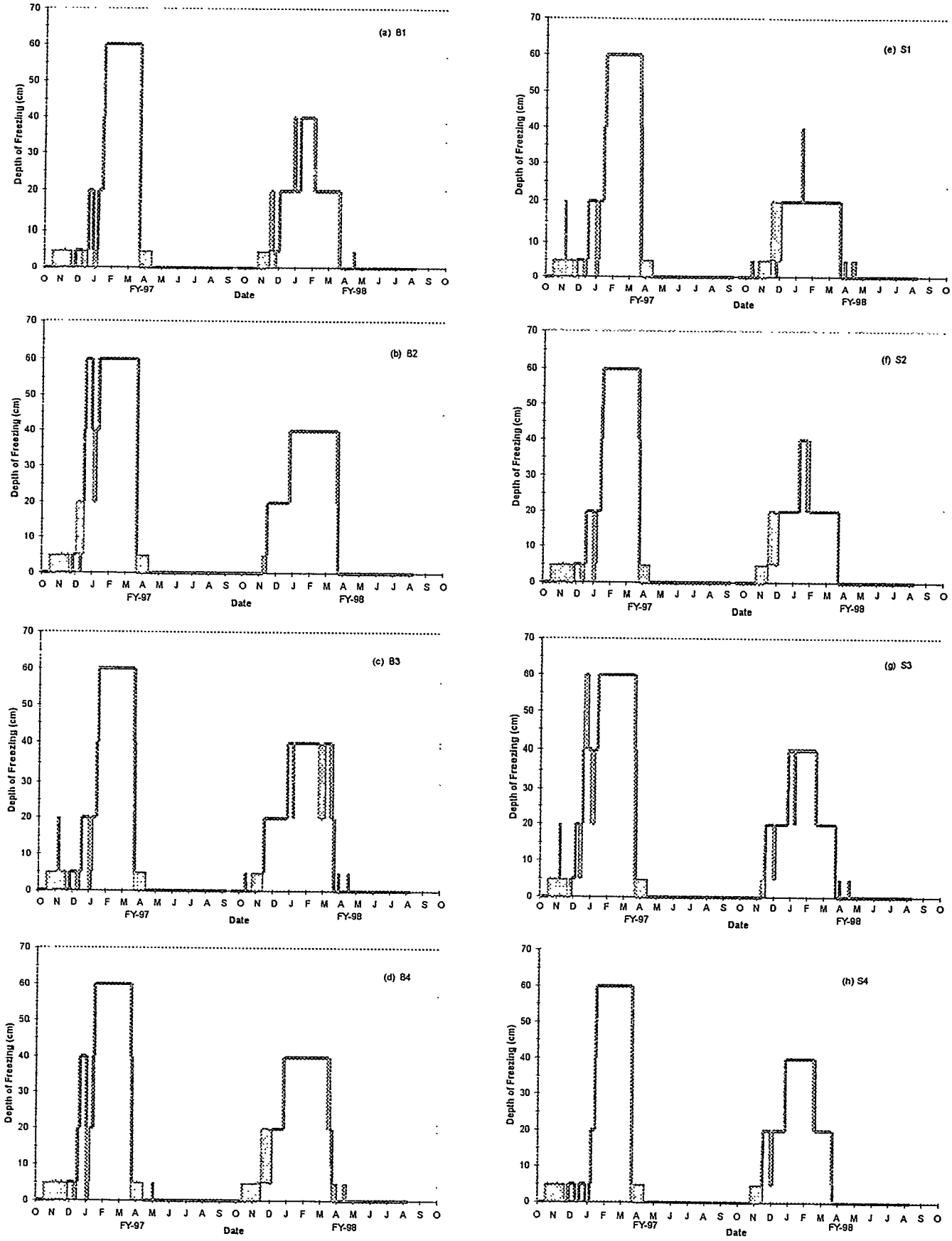

Figure 12. Depths of soil freezing during FY-97 and FY-98.

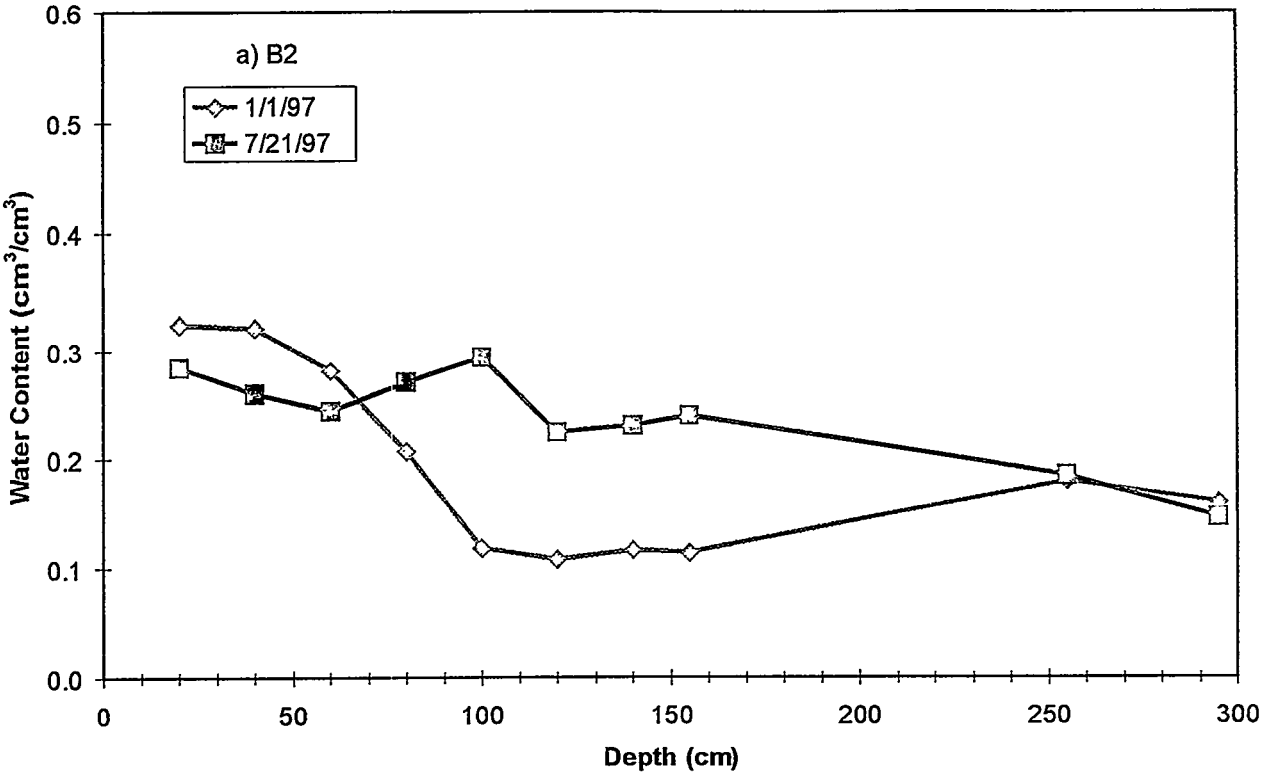

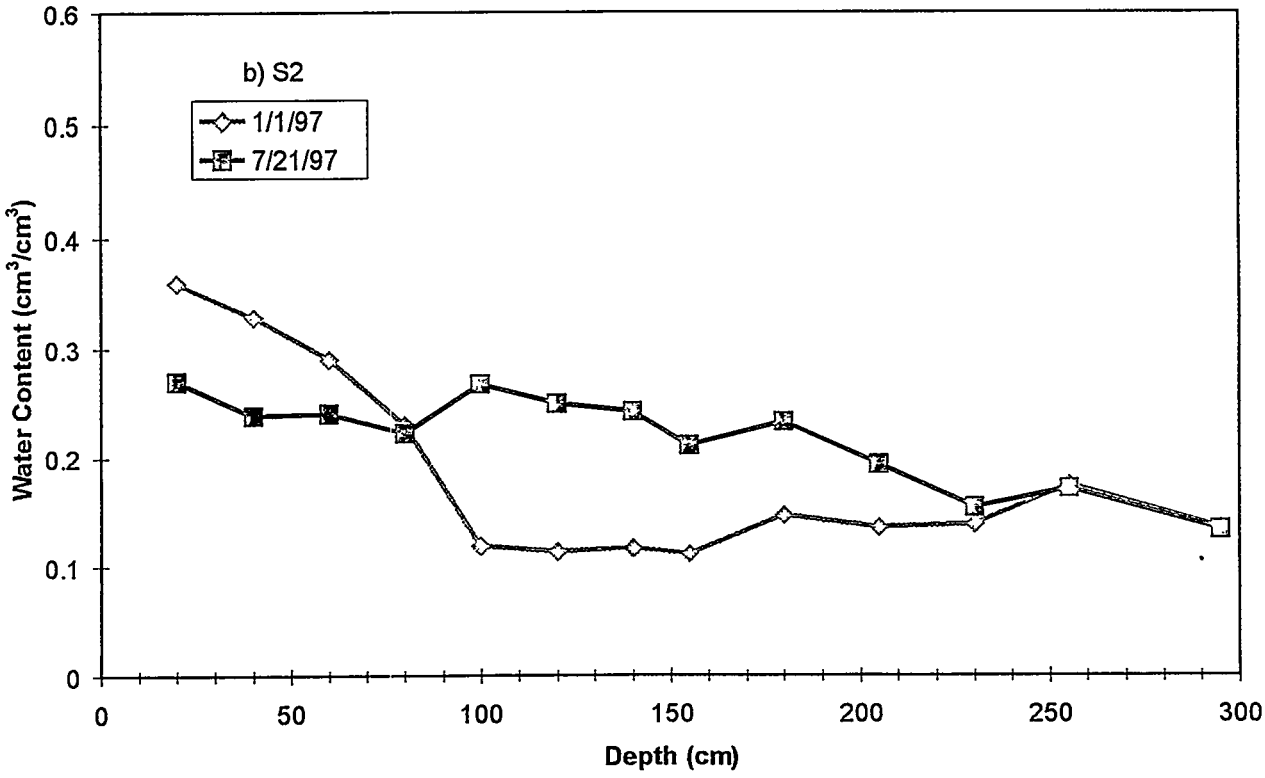

Figure 13. TDR-measured water content profiles in test plots B2 (a) and S2 (b).

storage until the winter of 1997-1998. From November to March, water storage is once again artificially depressed due to TDR probe measurements made in frozen soil. Note, however, that the amount of water stored did not decrease to pre-wetting test levels when drainage from the wetting tests practically ceased (see discussion in section 5.2) prior to winter 1998. This indicates that the test plot soils had significant reserve capacity for storing water when the wetting tests were initiated. This capacity was obviously less in the capillary/biobarrier test plots due to the presence of the 90-cm-thick barrier.

Another peak in water storage occurs in March of FY-98 as a result of infiltration during soil thawing. Melting snow on the soil surface combined with additional precipitation contributed to this peak, which was followed by drainage from all plots. As drainage leveled off, water storage continued to increase gradually, particularly in the thick soil plots. The capillary/biobarrier has the ability to keep water in the upper part of the plot (above the barrier) where it is more subject to evaporative losses. In the thick soil plots, water moves deeper into the plots where it is less subject to evaporative losses.

5.3 Drainage

Drainage, as discussed in this report, refers to water exiting the bottom of the test plots through the center or perimeter drains and measured in the corresponding sumps. No drainage occurred in FY-97 prior to the wetting tests. As stated above, the wetting tests were conducted in such a way as to guarantee that drainage would occur. Consequently, drainage was observed in all test plots within days of initiation of water application. Figure 14 shows the cumulative amounts of drainage from each plot through the end of calendar year 1997 as measured by both tipping buckets and pressure transducers. In general, drainage amounts correspond to amounts applied. More water was applied to plots S2 and S3 than plots B2 and B3, and, correspondingly, more water drained from plots S2 and S3 than from Plots B2 and B3. Comparable amounts of water were applied to plots B4 and S4 and the drainage was comparable. More water was applied to plot B1 than to S1, and more water drained from B1.

Figure 14 also shows that the initial, rapid drainage following the wetting tests slows down more abruptly in the capillary/biobarrier plots than in the thick soil plots (note the sharper curves in Figures 14a-d compared to Figures 14e-h). This is caused by the presence of the capillary/biobarrier. The capillary/biobarrier allows water to drain through it as long as soil at its upper boundary is saturated or very near saturation. When the soil water content drops below this level the barrier effectively stops further drainage. Soil water below the barrier can continue to drain. The capillary/biobarrier is absent in the thick soil test plots so water can continue to flow downward even under unsaturated conditions.

Ideally, the tipping bucket and pressure transducer measurements should yield equivalent amounts of drainage. Unfortunately, that is not the case for the drainage observed in Figure 14. The tipping bucket data generally shows less water drained than the pressure transducer data. Three factors likely contribute to the discrepancies observed between the two instruments. First, pressure transducer data collected at the EBTF is noisier than the tipping bucket data. However, the noise in the transducer data tends to cancel itself out so the effect of noise is probably minimal. Second, the four sumps draining the two test plots undergoing wetting were equipped with pumps to automatically empty the sumps when the water level reached a predetermined height. As stated above, wetting tests were conducted simultaneously on two plots at a given time. Typically, the wetting of subsequent plots was delayed a few days after a test to get by the initial rush of drainage so that the pumps could be moved to the next set of sumps. After moving the pumps, sumps from the initial set of tests continued to fill with water and had to be emptied manually. There were instances when the water level in those sumps rose high enough to disable the tipping bucket before the sumps could be emptied. Such instances were relatively rare and had minor influence on the

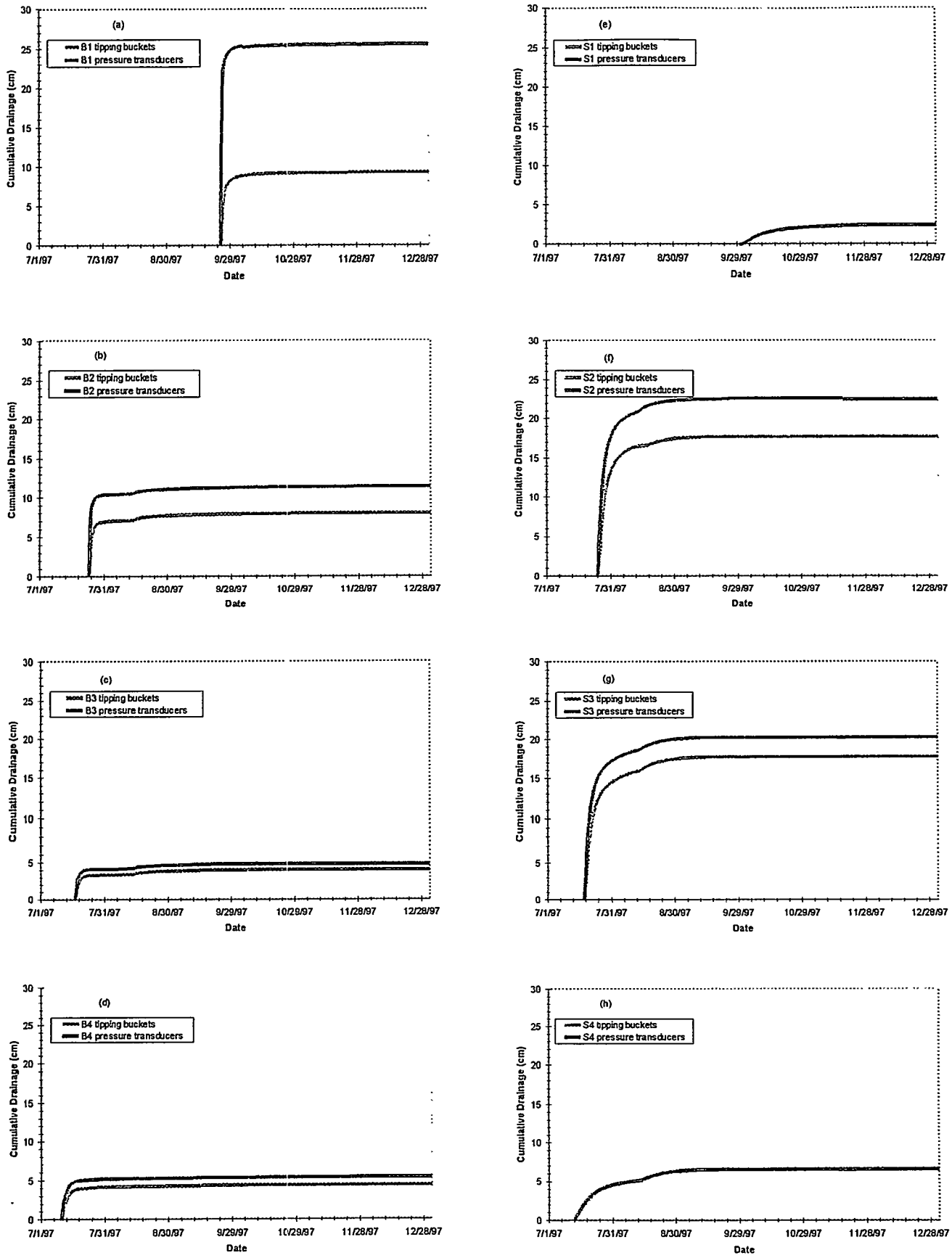

Figure 14. Cumulative drainage resulting from the FY-97 wetting tests.

amount of drainage. Tipping bucket data for such cases have been corrected using the pressure transducer data but discrepancies between the two instruments still remain. Third, and probably foremost, is the fact that the tipping buckets cannot handle high flow rates. The initial drainage from the wetting tests was fast enough to produce a steady stream of water that overflowed the buckets as they tipped from side to side. Most of the differences observed between the two instruments in Figure 14 occur early in the drainage pattern when the flow rate is fastest. The differences do not increase much as the flow rate slows down. Note also that in test plots S1 and S4 (Figures 14e and 14h, respectively) where less water was applied, there is less drainage, and the initial rate of drainage is less than in the other plots, as indicated by the less steep initial part of the drainage curve. The diminished initial drainage rates allowed the tipping buckets to function normally, thus producing data that agrees with the pressure transducer data.

The curves in Figure 14 indicate that drainage from the wetting tests had slowed to very low levels by the beginning of FY-98. This can be seen in more detail in Table 7, which shows total drainage from each test plot during the first five months of FY-98. Test plots B1 and S1 show noticeably more drainage than the other plots because wetting tests on these two plots were conducted in the latter half of September 1997 whereas wetting tests on the other plots were conducted in July. By February 1998, very little drainage is evident in test plots B1 and S1 and none whatsoever in the other test plots.

Drainage from all test plots resumed in mid-March 1998 (Figure 15). The resumption of drainage coincided with the thawing of frozen soil (Figure 12). Soil freezing can affect drainage in at least two ways. First, freezing can establish a barrier in the soil to subsequent infiltration of water from rainfall or snowmelt and to the downward flow of water. Second, freezing can immobilize water that is already in the soil, thus preventing its downward movement. This second mechanism was probably of little consequence during the winter of FY-98 because drainage had already slowed to very low levels by the time freezing started to reach the 20-cm depth in mid-November. The first mechanism played a much more significant role at the EBTF. Drainage in October 1997, before any significant freezing occurred, was already at much lower levels than the drainage that occurred in March 1998. Therefore, the March drainage must have had a source other than the wetting test water applications. That other source was precipitation during the late fall/winter of FY-98. Figures 5 to 7 indicate that precipitation occurred throughout this period and, with minor exceptions, the ground was covered with snow. As stated above, standing water under melting snow was observed on the test plots on March 16, 1998. By March 21, the next observation, all the snow had melted. Although drainage from the wetting tests had practically ceased prior to soil freezing, all of the test plots still held considerable amounts of water. This allowed the infiltrating water to move fairly rapidly through the plots and initiate drainage.

Figure 15 shows that drainage from the capillary/biobarrier plots again slows down more abruptly (note where the curves start to level out) than drainage from the thick soil test plots. This is consistent with the observations made of drainage immediately following the wetting tests (see Figure 14). Again, this characteristic is evidence of the effectiveness of the capillary/biobarrier in limiting drainage. Without the capillary/biobarrier, the thick soil plots continue to drain at higher rates and eventually allow more water to pass through the cover. This is evident also in Figure 11 where there is a greater decrease in water storage in the thick soil plots (Figures 11e to 11h) following the March peak than in the capillary/biobarrier plots (Figures 11a to 11d). Minimal evaporation at this time of the year coupled with no transpiration means that the water lost in the plots was drainage. Note also that discrepancies between cumulative drainage as measured by tipping buckets and pressure transducers as shown in Figure 14 are smaller than those seen in Figure 13. This is a result of the slower rates of drainage following the spring thaw than immediately following the wetting tests.

Table 7. Drainage amounts during late fall and winter of FY-98.

	Drainage[a] (cm)				
Plot	Oct-97	Nov-97	Dec-97	Jan-98	Feb-98
B1	0.6460	0.0570	0.0130	0.0036	0.0009
S1	2.1940	0.2260	0.0130	0.0004	0
B2	0.0730	0.0110	0.0010	0	0
S2	0	0	0	0	0
B3	0.0400	0	0	0	0
S3	0	0	0	0	0
B4	0.0530	0.0110	0	0	0
S4	0.0180	0.0010	0	0	0

a From tipping bucket data.

In the long term employment of engineered barriers, the most likely input of water to the barriers is precipitation. Therefore, it is of interest to compare the amount of drainage to the amount of precipitation. Figure 12 revealed that the soil began to freeze in November 1997 and Table 7 indicated that drainage from the wetting tests had practically ceased at that time. Assuming that the frozen soil prohibited infiltration, drainage beginning with the March 1998 thaw and continuing until the end of FY-98 can be attributed to precipitation falling on the test plots from November onward. Table 8 shows that drainage from the thick soil test plots was about double that from the capillary/biobarrier test plots even though the amount of precipitation was the same. Approximately one-third of the precipitation occurring during this period drained through the capillary/biobarrier test plots compared to two-thirds of the precipitation in the thick soil test plots.

The differences in drainage that are evident between the capillary/biobarrier and thick soil test plots appear to be the result of the fundamental differences between plot designs and not artifacts of testing the barriers in enclosed cells. The amount of drainage in the perimeter drains in all cases is less than the amount of drainage in the center drains. Table 9 shows that the ratio of perimeter drainage to center drainage is on the order of the perimeter-to-center drainage area ratio (0.15). Drainage in the perimeter drains was typically less than 0.5 L/hr following the FY-98 thaw. Drainage is not limited to this rate in the perimeter drains due to their size. Higher rates were observed in the perimeter drains immediately following the wetting tests in FY-97. Finally, the patterns of drainage in the perimeter drains match the patterns in the center drains. The drainage patterns of water bypassing the plot and flowing down the sidewalls would likely be different than that of water that has to flow through the soil.

5.4 Evaporation

Evaporation from the test plots was determined by rearranging Equation 10 and solving for ET, evapotranspiration. Transpiration during FY-97 and FY-98 was zero because all test plots were kept cleared of vegetation. The ET term, therefore, represents just evaporation, E. With the exception of evaporation, all terms in the equation are actually measured.

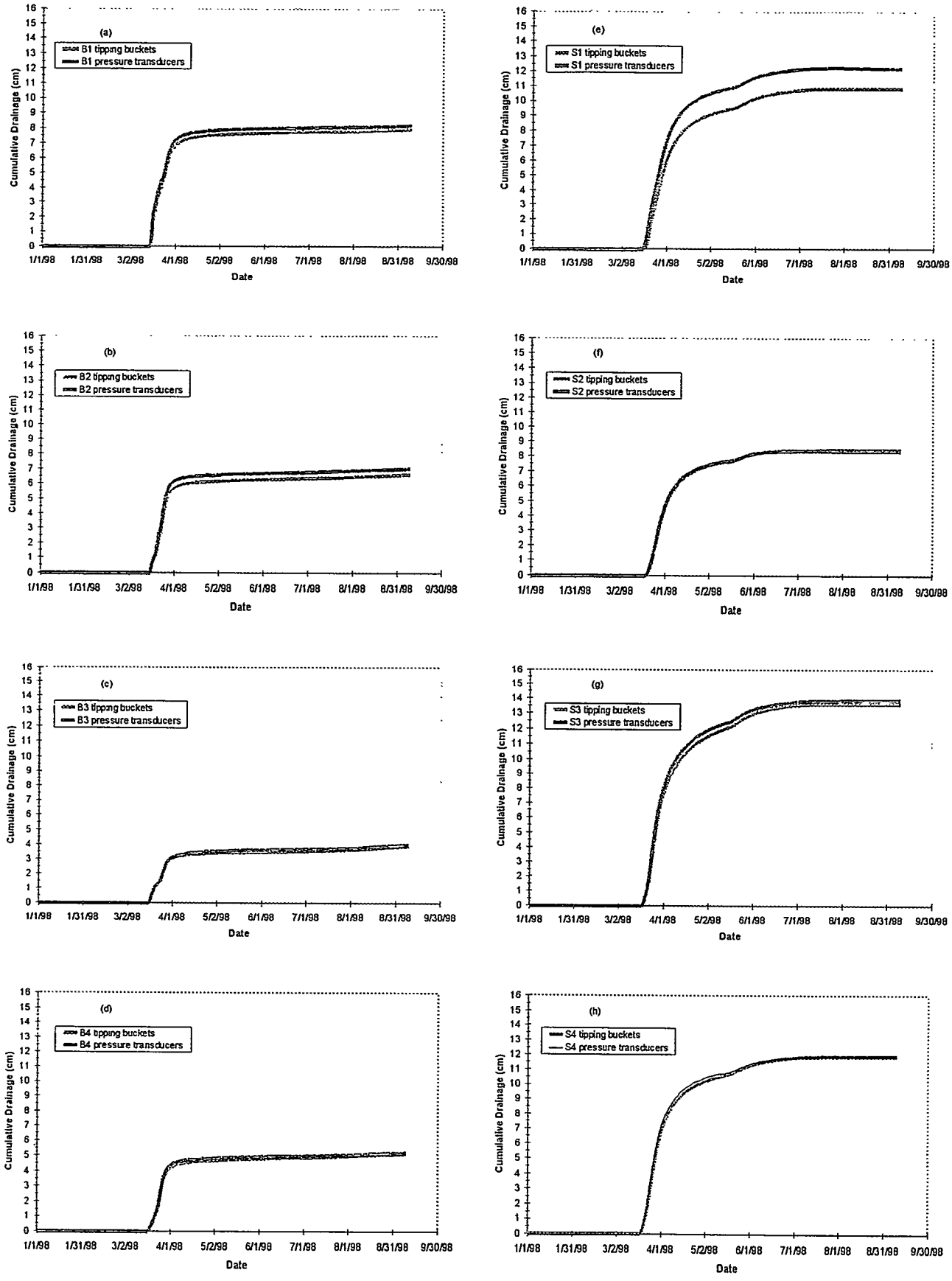

Figure 15. Cumulative drainage following the winter of FY-98.

Table 8. Drainage amounts and drainage as a percentage of precipitation in FY-98.

Plot	Tipping Bucket (cm)	Pressure Transducer (cm)
B1	8.02	8.31
B2	6.65	7.11
B3	3.89	4.03
B4	5.17	5.30
Average of "B" plots	5.93	6.19
% of total precipitation[a]	33.73	35.21
S1	11.06	12.49
S2	8.41	8.19
S3	13.61	13.90
S4	11.87	11.91
Average of "S" plots	11.24	11.62
% of total precipitation[a]	63.93	66.09

a. Total precipitation equals 17.582 cm from 11-1-97 to 9-9-98.

Table 9. Comparison of drainage from center and perimeter drains.

	Drainage from Spring Thaw to 8-17-98		
Plot	Center Tipping Bucket (L)	Perimeter Tipping Bucket (L)	Perimeter/Center
B1	515.8	180.8	0.35
B2	501.7	85.8	0.17
B3	300.1	49.4	0.16
B4	337.8	104.8	0.31
S1	879.5	125.7	0.14
S2	600.4	169.1	0.28
S3	1144.3	83.4	0.07
S4	924.4	178.1	0.19

Evaporation and the values used to calculate it are shown in Table 10. The negative value for evaporation for test plot S1 in FY-97 stands out as an anomaly. It is unclear why this value is negative; therefore, it is excluded from further discussions. On average, evaporation from the capillary/biobarrier test plots is greater than evaporation from the thick soil test plots in both FY-97 and FY-98 (21.65 cm and 16.21 cm vs. 10.39 cm and 6.12 cm). This observation is consistent with the other factors of the water balance equation discussed above. Drainage from the capillary/biobarrier test plots has been observed to cease prior to drainage from the thick soil test plots even when equal amounts of infiltration have occurred. Water that is redistributed downward and contributes to drainage in the thick soil plots is held in the upper portions of the capillary/biobarrier plots because the capillary/biobarrier effectively prohibits downward water flow when the water content of the soil at its upper interface is reduced to a level below saturation. The closer water is to the surface, the more it is subject to the evaporative forces of the atmosphere. Consequently, greater evaporation is observed from the capillary/biobarrier test plots than from the thick soil test plots.

Evaporation within each type of test plot was similar between the two years examined because the soils were wetted to similar degrees both years, i.e., both years included single infiltration events that were sufficient to yield drainage. In FY-97 this resulted from the input of significant amounts of water during the wetting tests. In FY-98, there were no wetting tests and less water infiltrated but the soils already contained significant amounts of water as a result of the wetting tests, so conditions were similar. However, as a percentage of precipitation (precipitation plus irrigation in FY-97), evaporation differed significantly between FY-97 and FY-98. In the capillary/biobarrier test plots, evaporation represented 89% of precipitation in FY-98 but only 31% of precipitation (plus irrigation) in FY-97. In the thick soil test plots, evaporation represented 32% of precipitation in FY-98 but only 12% of precipitation (plus irrigation) in FY-97. The lower percentages in FY-97 result from the fact that much of the water that infiltrated ended up filling empty storage capacity in the plots, particularly in the lower reaches of the plots where the bottom drains also serve as barriers to flow at less than saturated conditions and where water is out of reach of evaporative forces (see Figure 16).

5.5 Summary and Conclusions

The instrumentation installed at the EBTF was monitored throughout FY-97 and FY-98. Data collected from the instruments were used to evaluate the water balance components of the test plots for these two years. The water balance analysis revealed that wetting tests performed during FY-97 highlighted significant differences between the performance of the capillary/biobarrier and thick soil test plots both during the tests and in the following fiscal year.

The test plots received from 35.36 cm to 70.50 cm of water within a few days during the wetting tests. This is significantly greater than the average annual precipitation at the site (22.5 cm) and larger than any single storm event that is likely to occur at the site. Although continuous ponding of water on the soil surface was generally avoided during the wetting tests, these water applications are closer to representing flood conditions than just sporadic storm events. These wetting tests were intentionally designed to stress the engineered barrier test plots to the extreme so their performance during and particularly after the tests could be observed.

The capillary/biobarriers effectively halted drainage from the wetting tests sooner than the thick soil barriers and, thus, reduced the total amount of drainage that occurred. Similar results were observed in drainage data collected in FY-98 following the spring thaw. By limiting drainage, the capillary/biobarriers increased water storage in the upper portions of the test plots compared to the thick soil barriers. This led

Table 10. Evapotranspiration and other water balance components for FY-97 and FY-98.

Plot	FY	Beginning Storage[a] (cm)	Ending Storage[a] (cm)	ΔS (cm)	Precipitation (cm)	Irrigation (cm)	Drainage[b] (cm)	ET (cm)
B1	1997	38.23	83.54	45.31	24.3986	62.59	25.15	16.53
	1998[c]	83.53	81.03	-2.50	19.13	0	8.71	12.92
S1	1997	41.96	104.45	62.49	24.3986	35.36	0.000431	-2.73
	1998[c]	104.34	101.48	-2.86	19.13	0	14.68	7.31
B2	1997	46.50	76.38	29.88	24.3986	48.43	11.35	31.60
	1998[c]	76.49	74.84	-1.65	19.13	0	7.16	13.62
S2	1997	42.40	106.75	64.35	24.3986	70.50	22.69	7.86
	1998[c]	106.69	109.31	2.62	19.13	0	8.18	8.33
B3	1997	29.49	75.14	45.65	24.3986	42.02	4.835	15.93
	1998[c]	75.25	73.55	-1.70	19.13	0	4.03	16.80
S3	1997	49.67[d]	108.18	58.51	24.3986	69.31	20.28	14.92
	1998[c]	108.41	110.52	2.11	19.13	0	13.86	3.16
B4	1997	40.03[e]	75.52[e]	35.49	24.3986	39.01	5.365	22.55
	1998[c]	75.52[e]	67.81	-7.71	19.13	0	5.35	21.49
S4	1997	53.09[d]	104.91	51.82	24.3986	42.37	6.565	8.38
	1998[c]	105.09	106.63	1.54	19.13	0	11.91	5.68

a. Assumes the capillary/biobarrier holds no water.
b. From pressure transducers.
c. Data up to 9-09-98.
d. Less than 39 values.
e. Less than 30 values.

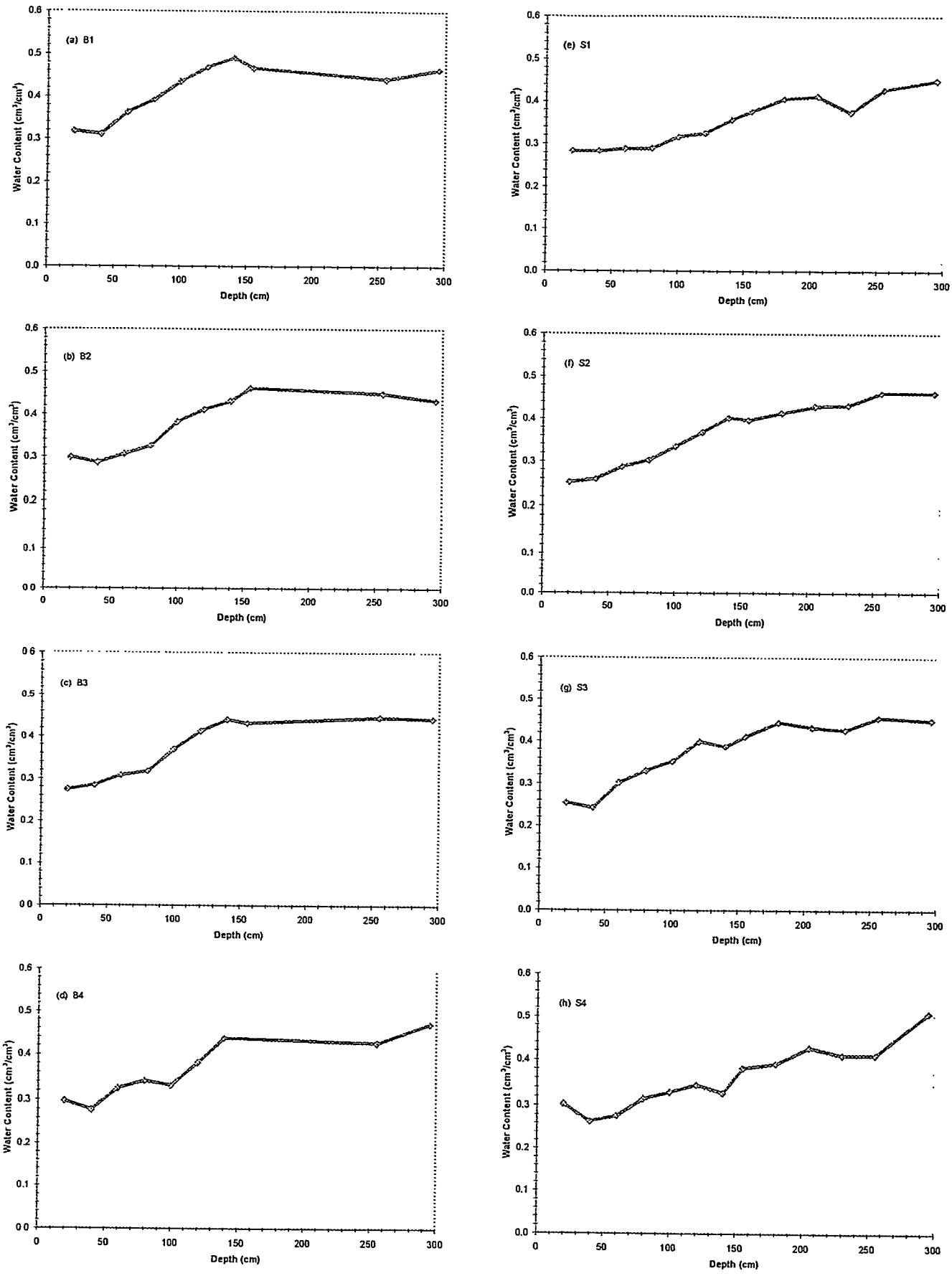

Figure 16. Soil water content profiles on October 1, 1997.

to increased recycling of water to the atmosphere through evaporation. Without vegetation on the test plots to help recycle stored water back to the atmosphere, however, all test plots showed gradual gains in water storage during FY-97 and FY-98. Prior to the wetting tests, none of the test plots produced drainage as a result of exposure to ambient conditions, and differences in the performance of the two barrier designs were revealed only in the internal distribution of water within the plots.

The capillary/biobarrier test plots also maintained their initial structure better in response to the large inputs of water during the wetting test than the thick soil test plots. Although soil subsidence was observed in all test plots, subsidence was significantly greater in the thick soil test plots than in the capillary/biobarrier test plots.

6. FUTURE TESTING

Monitoring of the EBTF test plots is scheduled to continue in order to evaluate further the response of the covers to the wetting tests. Vegetation will be established on the plots in 1999. Transpiration of water in the soil by plants will complement the other characteristics of the barriers that are already in place, i.e., the water storage ability of the soil and flow-stopping ability of the capillary barriers, in order to limit infiltration through the cover. Continued monitoring of the test plots will provide data to compare the covers under fully-functioning, ideal (vegetated) conditions to less-than-ideal (bare surface) conditions. Supplemental irrigation will be initiated on selected plots to evaluate the long-term performance of the covers under more severe (wetter) conditions than normally experienced at the SDA. Additional short-term stresses, e.g., 100-year storm, also will be simulated and evaluated. Upon conclusion of field testing, soil samples will be collected from selected test plots in order to characterize and evaluate changes in the physical and hydraulic properties of the covers over time. Field testing will be complemented with numerical modeling. Monitoring data will be used to calibrate and validate water flow models that can be used to predict the future performance of the covers being tested and evaluate other cover designs.

7. REFERENCES

Bishop, C. W., 1996, *Soil Moisture Monitoring Results at the Radioactive Waste Management Complex of the Idaho National Engineering Laboratory, FY-96, FY-95, FY-94*, INEL-96/297, Lockheed Martin Idaho Technologies Company, Idaho Falls, ID.

D. B. Stephens and Associates, Inc., June 1997a, *Hydraulic Properties of Lockheed Martin Idaho Technologies Company Soil Samples*, Albuquerque, New Mexico.

D. B. Stephens and Associates, Inc., July 1997b, *Hydraulic Properties of Lockheed Martin Idaho Technologies Company Soil Samples*, Albuquerque, New Mexico.

D. B. Stephens and Associates, Inc., 1996, *Calibration of Heat Dissipation and Thermocouple Psychrometer Probes*, Albuquerque, New Mexico.

Bragassa, P.W., 1994, *A-E Construction Specification: RWMC SDA Engineered Barriers Test Facility Title I Design*, A-ECS 40705, EG&G Idaho, Inc., Idaho Falls, ID.

Bragassa, P.W., 1995, *A-E Construction Specification: SDA Engineered Barriers Test Facility Title II Design*, A-ECS 40705, EG&G Idaho, Inc., Idaho Falls, ID.

Dunne, T. and L. B. Leopold, 1978, *Water in Environmental Planning*, W. H. Freeman & Company, San Francisco, CA.

Eastman, R. L., J. A. Hackney, J. F. Keck, R. G. Street, and T. C. Wheeler, 1992, *Idaho National Engineering Laboratory Radioactive Waste Management Complex Subsurface Disposal Area Engineered Barriers Final Design (Title II)*, Project File No. 020618, EG&G Idaho, Inc., Idaho Falls, ID.

Kaser, T. G., and M. K. Adler Flitton, 1997, *Data Acquisition System for RWMC SDA Engineered Barriers Test*, INEL-96/311, Lockheed Martin Idaho Technologies Company, Idaho Falls, Idaho.

Keck, J. F., 1992, *Evaluation of Engineered Barriers For Closure Cover of the Radioactive Waste Management Complex Subsurface Disposal Area*, EDF# RWMC-523, EG&G Idaho, Inc., Idaho Falls, ID.

Magnuson, S. O., 1993, *A Simulation Study of Moisture Movement in Proposed Barriers for the Subsurface Disposal Area, INEL*, EGG-WM-10974, EG&G Idaho, Inc., Idaho Falls, ID.

Maheras, S. J., A. S. Rood, S. O. Magnuson, M. E. Sussman, and R. N. Bhatt, 1994, *Radioactive Waste Management Complex Low-Level Waste Radiological Performance Assessment*, EGG-WM-8773, EG&G Idaho, Inc., Idaho Falls, ID.

Porro, I., and K. N. Keck, 1997, *Summary of Activities at the Engineered Barriers Test Facility, October 1, 1995, to January 31, 1997, and Initial Data*, INEEL/EXT-97-00239, Lockheed Martin Idaho Technologies Company, Idaho Falls, Idaho.

Porro, I., and K. N. Keck, 1996, *RWMC SDA Engineered-Barrier Test Operating Procedures*, INEL-96/0205, Lockheed Martin Idaho Technologies Company, Idaho Falls, Idaho.

Porro, I., K. N. Keck, D. L. McElroy, and C. W. Bishop, 1996, *RWMC SDA Engineered-Barrier Test Plan*, INEL-96/0003, Lockheed Martin Idaho Technologies Company, Idaho Falls, Idaho.

Topp, G. C., J. L. Davis, and A. P. Annan, 1980, "Electromagnetic Determination of Soil Water Content: Measurements in Coaxial Transmission Lines," *Water Resources Research*, 16(3), pp. 574-582.

Appendix A

Soil Properties Data and Methods of Analysis

Table 1. Soil properties and methods of analysis.

Soil Properties	Methods of Analysis
Saturated hydraulic conductivity	MOSA[a], Part 1, Chapter 28; or ASTM[b] D 2434; or ASTM D 5084
Initial volumetric water content	MOSA, Part 1, Chapter 21
Dry bulk density	MOSA, Part 1, Chapter 13 or ASTM D 2937-94
Calculated total porosity	MOSA, Part 1, Chapter 18, Section 2.1.1
Moisture characteristic (7 points)	MOSA, Part 1, Chapters 24 & 26; or ASTM D 3152
Calculated unsaturated hydraulic conductivity	SSSAJ[c], 1980
Standard sieves #4 to #200 and hydrometer	ASTM D 422-63
Atterberg limits	ASTM D 4318-93
Particle density/specific gravity	ASTM D 854-92

a. Methods of Soil Analysis, Part 1, 1986, A. Klute, ed., American Society of Agronomy, Madison, WI.
b. American Society for Testing and Materials Annual Book of Standards.
c. Soil Science Society of America Journal, 1980, Vol. 44, pp. 892-898.

Table 2. Summary of initial moisture content, dry bulk density, wet bulk density, and calculated porosity.

Sample Number	Initial Moisture Content		Dry Bulk Density	Wet Bulk Density	Calculated Porosity
	Gravimetric (%, g/g)	Volumetric (%, cm^3/cm^3)	(g/cm^3)	(g/cm^3)	(%)
D30C1	16.8	23.8	1.42	1.66	47.4
D30C2	18.2	24.8	1.36	1.61	49.8
D30C3	18.2	25.8	1.41	1.67	47.2
D60C1	18.6	25.9	1.39	1.65	48.4
D60C2	18.6	26.8	1.44	1.71	46.4
D60C3	18.4	26.3	1.42	1.69	47.0
D90C1	18.3	25.9	1.42	1.67	47.8
D90C2	17.6	26.8	1.52	1.79	43.6
D90C3	15.7	23.4	1.49	1.73	44.6
D120C1	15.9	23.2	1.45	1.69	46.3
D120C2	15.8	24.4	1.55	1.79	43.2
D120C3	15.3	22.6	1.48	1.71	44.6
D150C1	17.1	26.7	1.56	1.83	41.6
D150C2	17.7	24.8	1.40	1.65	47.8
D150C3	17.1	25.8	1.50	1.76	43.9
D180C1	17.3	24.9	1.44	1.69	46.7
D180C2	18.3	25.5	1.39	1.65	48.1
D180C3	17.4	25.7	1.47	1.73	45.2
D210C1	16.9	24.4	1.45	1.69	46.2
D210C2	17.3	26.1	1.50	1.76	44.1
D210C3	17.2	27.1	1.57	1.85	41.5
D240C1	16.2	22.7	1.40	1.63	47.8
D240C2	16.7	24.8	1.48	1.73	44.9
D240C3	16.8	23.9	1.42	1.66	47.1
D250C1	16.0	23.3	1.45	1.69	46.3
D250C2	16.2	22.0	1.36	1.58	49.8
D250C3	15.9	22.7	1.43	1.66	47.1
D270C1	16.6	23.0	1.39	1.61	48.1
D270C2	17.0	26.6	1.56	1.83	41.5
D270C3	16.4	25.8	1.57	1.83	41.7
D500C1	9.2	12.5	1.36	1.49	49.6
D500C2	5.6	8.6	1.52	1.60	43.8
D500C3	5.4	8.3	1.53	1.61	42.8
I510C1	13.8	20.3	1.47	1.67	45.3
I560C1	18.1	27.0	1.49	1.76	44.5
I590C1	18.4	27.2	1.48	1.75	44.9
I5120C1	20.9	32.6	1.56	1.89	42.3
I5150C1	19.1	28.7	1.50	1.79	44.1
I5180C1	16.9	24.0	1.42	1.66	47.6

Table 3. Summary of moisture characteristics of the initial drainage curve.

Sample Number	Pressure Head (-cm water)	Moisture Content (%, cm^3/cm^3)
D30C1	0	49.1
	20	46.4
	59	44.8
	142	37.9
	510	28.5
	3263	22.6
	14991	17.2
D30C2	0	48.1
	25	41.8
	50	38.4
	153	31.7
	510	27.3
	2855	21.5
	16521	15.7
D30C3	0	49.1
	20	45.6
	53	41.3
	153	36.2
	510	30.2
	3161	22.2
	18560	16.6
D60C1	0	46.8
	22	44.0
	50	41.8
	153	35.3
	510	28.3
	3365	20.7
	16113	17.4
D60C2	0	49.8
	22	45.8
	51	44.1
	153	36.0
	510	28.5
	3365	21.2
	17847	16.5
D60C3	0	48.0
	21	45.9
	50	41.9
	147	34.3
	510	27.0
	3161	22.1
	16725	14.0
D90C1	0	49.1
	23	44.7
	51	40.8

Table 3. (continued).

Sample Number	Pressure Head (-cm water)	Moisture Content (%, cm^3/cm^3)
	153	36.2
	510	30.1
	3161	23.3
	14379	17.6
D90C2	0	44.2
	24	41.8
	50	40.9
	153	35.4
	510	30.0
	4589	20.3
	16113	17.2
D90C3	0	47.4
	23	45.3
	49	45.0
	148	37.5
	510	28.8
	3161	21.5
	14787	16.9
D120C1	0	50.7
	20	46.1
	51	44.8
	153	38.8
	510	30.6
	3569	22.9
	16113	17.8
D120C2	0	47.1
	21	44.2
	51	41.9
	152	36.7
	510	30.0
	5507	22.4
	13971	18.3
D120C3	0	50.1
	21	48.0
	51	46.2
	149	39.3
	510	30.0
	4181	22.5
	14685	18.3
D150C1	0	47.0
	25	43.1
	51	41.8
	153	36.0
	510	28.9
	3773	24.8
	15603	18.9

Table 3. (continued).

Sample Number	Pressure Head (-cm water)	Moisture Content (%, cm^3/cm^3)
D150C2	0	50.2
	21	48.9
	50	45.3
	154	35.9
	1530	29.3
	4385	20.4
	15909	15.3
D150C3	0	46.6
	23	47.7
	50	41.7
	153	37.9
	510	31.5
	3161	25.1
	15093	20.0
D180C1	0	47.1
	22	45.6
	51	41.0
	153	35.6
	510	28.7
	3569	23.9
	17031	16.9
D180C2	0	49.8
	20	45.7
	50	42.3
	153	36.7
	510	29.8
	3161	23.2
	16623	15.6
D180C3	0	49.9
	22	44.3
	53	42.4
	153	36.4
	510	30.9
	3875	23.1
	14685	17.6
D210C1	0	49.5
	23	44.8
	51	42.9
	153	37.1
	510	30.3
	4589	26.8
	17235	18.9
D210C2	0	47.2
	20	44.6
	51	43.6

Table 3. (continued).

Sample Number	Pressure Head (-cm water)	Moisture Content (%, cm^3/cm^3)
	153	37.1
	510	30.9
	4283	23.0
	15297	18.5
D210C3	0	44.7
	22	42.3
	51	41.5
	153	38.1
	510	32.2
	3467	24.2
	17948	18.0
D240C1	0	50.2
	23	47.7
	51	42.5
	153	38.4
	510	29.3
	3161	23.0
	15603	16.5
D240C2	0	46.7
	23	44.6
	54	43.6
	153	36.6
	510	30.5
	4181	22.2
	17745	17.4
D240C3	0	48.1
	21	44.0
	51	42.2
	153	35.9
	510	29.9
	2957	16.1
	16113	13.6
D250C1	0	47.3
	25	42.9
	52	41.5
	153	35.2
	510	28.6
	3977	21.7
	12849	17.1
D250C2	0	45.0
	22	42.6
	55	41.1
	153	33.8
	510	26.7
	3263	21.7
	16725	16.6

Table 3. (continued).

Sample Number	Pressure Head (-cm water)	Moisture Content (%, cm^3/cm^3)
D250C3	0	48.6
	21	45.8
	50	44.3
	153	38.2
	510	29.6
	3467	21.2
	14379	17.8
D270C1	0	48.5
	22	43.2
	51	40.0
	153	37.3
	510	30.5
	3365	22.6
	17541	16.3
D270C2	0	47.2
	23	42.9
	51	39.6
	153	36.4
	510	30.4
	3671	22.0
	19070	17.5
D270C3	0	45.0
	19	43.0
	51	42.1
	153	36.6
	510	31.2
	3059	25.7
	16725	18.0
D500C1	0	48.5
	21	45.9
	51	38.8
	153	33.6
	510	24.6
	3365	19.9
	20192	13.6
D500C2	0	44.0
	21	38.9
	51	36.4
	153	30.1
	510	23.0
	2753	18.5
	17541	12.2
D500C3	0	44.0
	21	41.9
	51	38.5

Table 3. (continued).

Sample Number	Pressure Head (-cm water)	Moisture Content (%, cm^3/cm^3)
	153	31.2
	510	23.6
	2753	18.4
	16215	12.9
I510C1	0	45.8
	22	43.2
	51	42.4
	153	36.0
	510	28.9
	3365	21.4
	15807	17.1
I560C1	0	42.7
	24	41.9
	51	40.2
	153	35.1
	510	29.2
	4487	22.1
	15603	18.1
I590C1	0	48.1
	25	45.7
	53	42.0
	153	37.1
	510	31.0
	3263	24.8
	16011	20.0
I5120C1	0	43.2
	25	40.6
	125	35.4
	510	31.0
	4283	23.2
	7343	19.7
	15093	17.2
I5150C1	0	43.3
	21	42.8
	50	41.5
	153	36.1
	510	30.4
	3977	20.7
	17948	16.9
I5180C1	0	48.3
	23	44.5
	50	43.0
	153	37.0
	510	29.9
	3773	20.5
	14787	17.8

Table 4. Summary of calculated unsaturated hydraulic properties.

Sample Number	α (cm^{-1}) Calculated Value	α (cm^{-1}) 95% Confidence Limits Lower	α (cm^{-1}) 95% Confidence Limits Upper	N (dimensionless) Calculated Value	N (dimensionless) 95% Confidence Limits Lower	N (dimensionless) 95% Confidence Limits Upper	θ_r (%)	θ_s (%)
D30C1	0.0133	-0.0019	0.0285	1.4173	0.9437	1.8909	0.1408	0.4875
D30C2	0.0704	0.0068	0.1341	1.1724	1.0244	1.3203	0.0254	0.4818
D30C3	0.0380	0.0321	0.0438	1.1650	1.1590	1.1710	0.0000	0.4910
D60C1	0.0179	0.0113	0.0245	1.3366	1.2228	1.4504	0.1214	0.4657
D60C2	0.0213	0.0040	0.0386	1.3149	1.0880	1.5418	0.1071	0.4951
D60C3	0.0280	-0.0235	0.0795	1.2399	0.8272	1.6525	0.0522	0.4850
D90C1	0.0459	0.0286	0.0631	1.1539	1.1406	1.1671	0.0000	0.4909
D90C2	0.0154	0.0026	0.0281	1.2206	1.0112	1.4299	0.0568	0.4400
D90C3	0.0109	0.0023	0.0196	1.4412	1.0938	1.7887	0.1378	0.4733
D120C1	0.0244	-0.0100	0.0587	1.2037	0.9042	1.5032	0.0417	0.5009
D120C2	0.0257	-0.0039	0.0553	1.1925	0.9460	1.4390	0.0552	0.4699
D120C3	0.0125	0.0031	0.0220	1.4225	1.1089	1.7360	0.1498	0.4989
D150C1	0.0291	-0.0264	0.0846	1.2255	0.8036	1.6474	0.1060	0.4695
D150C2	0.0249	-0.0190	0.0687	1.1862	1.1089	1.2634	0.0000	0.5083
D150C3	0.0224	0.0046	0.0401	1.1797	1.0167	1.3426	0.0579	0.4664
D180C1	0.0282	-0.0260	0.0824	1.2208	0.8095	1.6320	0.0766	0.4757
D180C2	0.0346	0.0136	0.0556	1.1724	1.1471	1.1977	0.0000	0.4957
D180C3	0.0433	0.0160	0.0706	1.1541	1.1320	1.1762	0.0000	0.4956
D210C1	0.0555	-0.0331	0.1440	1.1299	1.0868	1.1730	0.0000	0.4961
D210C2	0.0178	-0.0029	0.0385	1.2351	0.9419	1.5283	0.0848	0.4707
D210C3	0.0118	0.0060	0.0176	1.1654	1.1438	1.1871	0.0000	0.4420
D240C1	0.0275	-0.0144	0.0694	1.2101	0.8875	1.5326	0.0385	0.5043
D240C2	0.0149	-0.0010	0.0307	1.2819	0.9762	1.5876	0.1019	0.4678
D240C3	0.0147	-0.0167	0.0460	1.2663	0.6798	1.8529	0.0199	0.4711
D250C1	0.0298	-0.0021	0.0617	1.1979	0.9684	1.4273	0.0430	0.4717
D250C2	0.0162	-0.0029	0.0353	1.3854	0.9675	1.8033	0.1365	0.4500
D250C3	0.0128	0.0047	0.0209	1.3750	1.1383	1.6116	0.1269	0.4808
D270C1	0.0366	0.0009	0.0723	1.1584	1.1225	1.1942	0.0000	0.4787
D270C2	0.0381	0.0144	0.0618	1.1489	1.1281	1.1697	0.0000	0.4689

Table 4. (continucd).

Sample Number	α (cm^{-1})			N (dimensionless)			θ_r (%)	θ_s (%)
	Calculated Value	95% Confidence Limits		Calculated Value	95% Confidence Limits			
		Lower	Upper		Lower	Upper		
D270C3	0.0180	0.0013	0.0348	1.1527	1.1173	1.1881	0.0000	0.4496
D500C1	0.0330	-0.0174	0.0834	1.2979	0.9231	1.6727	0.0850	0.4894
D500C2	0.0446	-0.0129	0.1021	1.1951	0.9607	1.4295	0.0069	0.4389
D500C3	0.0199	0.0051	0.0347	1.3557	1.1227	1.5887	0.0891	0.4414
I510C1	0.0139	0.0027	0.0252	1.3232	1.0649	1.5814	0.1120	0.4555
I560C1	0.0135	0.0014	0.0256	1.2831	1.0120	1.5541	0.1162	0.4299
I590C1	0.0269	0.0089	0.0450	1.2332	1.0817	1.3847	0.1126	0.4834
I5120C1	0.0185	-0.0013	0.0383	1.1525	1.1164	1.1887	0.0000	0.4285
I5150C1	0.0097	0.0035	0.0158	1.3066	1.0919	1.5213	0.0989	0.4358
I5180C1	0.0190	0.0011	0.0368	1.2686	1.0167	1.5206	0.0879	0.4784

Table 5. Summary of saturated hydraulic conductivity tests.

Sample Number	K_{sat} (cm/sec)	Method of Analysis	
		Constant Head	Falling Head
D30C1	4.8E-05	X	
D30C2	2.2E-04	X	
D30C3	1.2E-04	X	
D60C1	1.6E-04	X	
D60C2	1.2E-04	X	
D60C3	2.2E-04	X	
D90C1	3.4E-05		X
D90C2	2.3E-05		X
D90C3	9.8E-05	X	
D120C1	4.9E-05	X	
D120C2	1.8E-04	X	
D120C3	2.3E-04	X	
D150C1	2.2E-05	X	
D150C2	3.6E-04	X	
D150C3	2.7E-05	X	
D180C1	1.3E-04	X	
D180C2	1.7E-04	X	
D180C3	7.3E-05	X	
D210C1	1.6E-04	X	
D210C2	6.0E-05	X	
D210C3	1.3E-05	X	
D240C1	1.1E-04	X	
D240C2	3.6E-05	X	
D240C3	2.0E-05	X	
D250C1	6.1E-05	X	
D250C2	5.8E-05	X	
D250C3	7.9E-05	X	
D270C1	1.4E-04	X	
D270C2	2.0E-05		X
D270C3	2.4E-05	X	
D500C1	2.5E-04	X	
D500C2	2.7E-04	X	
D500C3	1.5E-04	X	
I510C1	3.9E-05	X	
I560C1	3.8E-05	X	
I590C1	9.4E-05	X	
I5120C1	3.5E-06		X
I5150C1	4.1E-05	X	
I5180C1	5.1E-05	X	

Table 6. Summary of particle size characteristics.

Sample Number	d_{10} (mm)	d_{50} (mm)	d_{60} (mm)	C_u	C_c	Method	Classification
D30G1	0.00035	0.020	0.029	83	4.2	WS/H	Lean clay
D30G2	0.00020	0.021	0.029	150	6.4	WS/H	Lean clay
D30G3	0.00030	0.019	0.026	87	2.6	WS/H	Lean clay
D60G1	0.00054	0.019	0.028	52	1.7	WS/H	Lean clay
D60G2	0.00016	0.019	0.028	180	5.1	WS/H	Lean clay
D60G3	0.00033	0.019	0.028	85	2.9	WS/H	Lean clay
D90G1	0.00052	0.020	0.028	54	2.5	WS/H	Lean clay
D90G2	0.00029	0.018	0.028	97	2.5	WS/H	Lean clay
D90G3	0.00039	0.016	0.024	62	1.8	WS/H	Lean clay
D120G1	0.00023	0.017	0.025	110	2.0	WS/H	Lean clay
D120G2	0.00027	0.020	0.028	100	4.8	WS/H	Lean clay
D120G3	0.00030	0.020	0.028	93	3.2	WS/H	Silt
D150G1	0.00028	0.019	0.028	100	1.8	WS/H	Silt
D150G2	0.00021	0.020	0.030	140	5.9	WS/H	Lean clay
D150G3	0.00034	0.018	0.027	79	2.3	WS/H	Lean clay
D180G1	0.00030	0.018	0.027	90	2.4	WS/H	Lean clay
D180G2	0.000064	0.020	0.030	470	14	WS/H	Lean clay
D180G3	0.00015	0.020	0.030	200	5.8	WS/H	Lean clay
D210G1	0.00035	0.020	0.028	80	2.4	WS/H	Lean clay
D210G2	0.00018	0.020	0.030	170	5.0	WS/H	Lean clay
D210G3	0.00025	0.018	0.026	100	3.7	WS/H	Lean clay
D240G1	0.00013	0.018	0.027	210	6.3	WS/H	Lean clay
D240G2	0.00018	0.019	0.027	150	5.4	WS/H	Lean clay
D240G3	0.000015	0.019	0.028	1900	69	WS/H	Lean clay
D250G1	0.00018	0.010	0.017	94	1.6	WS/H	Lean clay
D250G2	0.00036	0.021	0.032	89	2.7	WS/H	Lean clay
D250G3	0.00024	0.021	0.030	130	5.9	WS/H	Lean clay
D270G1	0.00016	0.018	0.028	180	5.6	WS/H	Lean clay
D270G2	0.00016	0.020	0.030	190	4.6	WS/H	Lean clay
D270G3	0.00011	0.022	0.033	300	9.6	WS/H	Lean clay w/ gravel

Table 6. (continued).

Sample Number	d_{10} (mm)	d_{50} (mm)	d_{60} (mm)	C_u	C_c	Method	Classification
D500G1	0.0012	0.045	0.078	65	2.7	WS/H	Gravelly lean clay
D500G2	0.00063	0.039	0.064	100	4.9	WS/H	Gravelly lean clay
D500G3	0.00086	0.043	0.067	78	3.4	WS/H	Gravelly lean clay
I510G1	0.00029	0.018	0.025	86	3.6	WS/H	Lean clay
I560G1	0.00025	0.019	0.028	110	3.3	WS/H	Lean clay
I590G1	0.00022	0.018	0.024	110	4.2	WS/H	Lean clay
I5120G1	0.00020	0.018	0.027	140	5.2	WS/H	Lean clay
I5150G1	0.00021	0.018	0.027	130	3.9	WS/H	Lean clay
I5180G1	0.00035	0.019	0.027	77	3.1	WS/H	Lean clay

Note: Reported values for d_{10}, C_u, C_c, and soil classification are estimates, since extrapolation was required to obtain the d_{10} diameter.
WS = Wet sieve
H = Hydrometer
d_{50} = Median particle diameter
$Cu = d_{60}/d_{10}$
$Cc = (d_{30})^2/(d_{10})(d_{60})$.

Table 7. Summary of particle density tests.

Sample Number	Particle Density (g/cm^3)
D30G1	2.70
D30G2	2.71
D30G3	2.68
D60G1	2.69
D60G2	2.69
D60G3	2.69
D90G1	2.71
D90G2	2.69
D90G3	2.69
D120G1	2.71
D120G2	2.72
D120G3	2.67
D150G1	2.67
D150G2	2.68
D150G3	2.68
D180G1	2.70
D180G2	2.69
D180G3	2.69
D210G1	2.69
D210G2	2.71
D210G3	2.69
D240G1	2.69
D240G2	2.69
D240G3	2.69
D250G1	2.71
D250G2	2.70
D250G3	2.71
D270G1	2.67
D270G2	2.67
D270G3	2.70
D500G1	2.71
D500G2	2.70
D500G3	2.67
I510G1	2.69
I560G1	2.68
I590G1	2.68
I5120G1	2.70
I5150G1	2.68
I5180G1	2.70

Table 8. Summary of Atterberg tests.

Sample Number	Liquid Limit	Plastic Limit	Plasticity Index	Classification
D30G1	30.6	20.6	10.1	Clay
D30G2	30.0	21.3	8.7	Clay
D30G3	32.1	21.0	11.0	Clay
D60G1	31.7	22.4	9.3	Clay
D60G2	31.9	18.2	13.7	Clay
D60G3	31.6	22.5	9.0	Clay
D90G1	30.4	22.1	8.3	Clay
D90G2	31.6	22.2	9.4	Clay
D90G3	31.1	20.9	10.2	Clay
D120G1	31.4	22.6	8.8	Clay
D120G2	33.9	21.0	12.8	Clay
D120G3	32.2	24.2	7.9	Silt
D150G1	32.3	25.1	7.2	Silt
D150G2	32.7	20.2	12.4	Clay
D150G3	33.4	21.1	12.3	Clay
D180G1	31.9	19.5	12.3	Clay
D180G2	32.3	18.9	13.4	Clay
D180G3	32.7	19.4	13.4	Clay
D210G1	32.4	19.9	12.5	Clay
D210G2	31.6	17.6	14.0	Clay
D210G3	33.0	18.9	14.1	Clay
D240G1	32.3	18.5	13.8	Clay
D240G2	31.9	22.9	9.1	Clay
D240G3	31.6	21.4	10.2	Clay
D250G1	31.8	20.2	11.6	Clay
D250G2	33.5	22.4	11.1	Clay
D250G3	30.9	20.6	10.3	Clay
D270G1	30.9	21.4	9.4	Clay
D270G2	31.6	20.2	11.5	Clay
D270G3	33.0	20.9	12.1	Clay
D500G1	31.3	21.3	10.0	Clay
D500G2	29.8	17.0	12.8	Clay
D500G3	30.5	18.9	11.6	Clay
I510G1	31.6	19.9	11.8	Clay
I560G1	32.1	22.2	10.0	Clay
I590G1	32.8	19.8	13.0	Clay
I5120G1	33.4	20.7	12.7	Clay
I5150G1	32.1	17.7	14.5	Clay
I5180G1	30.2	19.4	10.7	Clay